iScience

CellPress
OPEN ACCESS

Article

Citrate shuttling in astrocytes is required for processing cocaine-induced neuron-derived excess peroxidated fatty acids

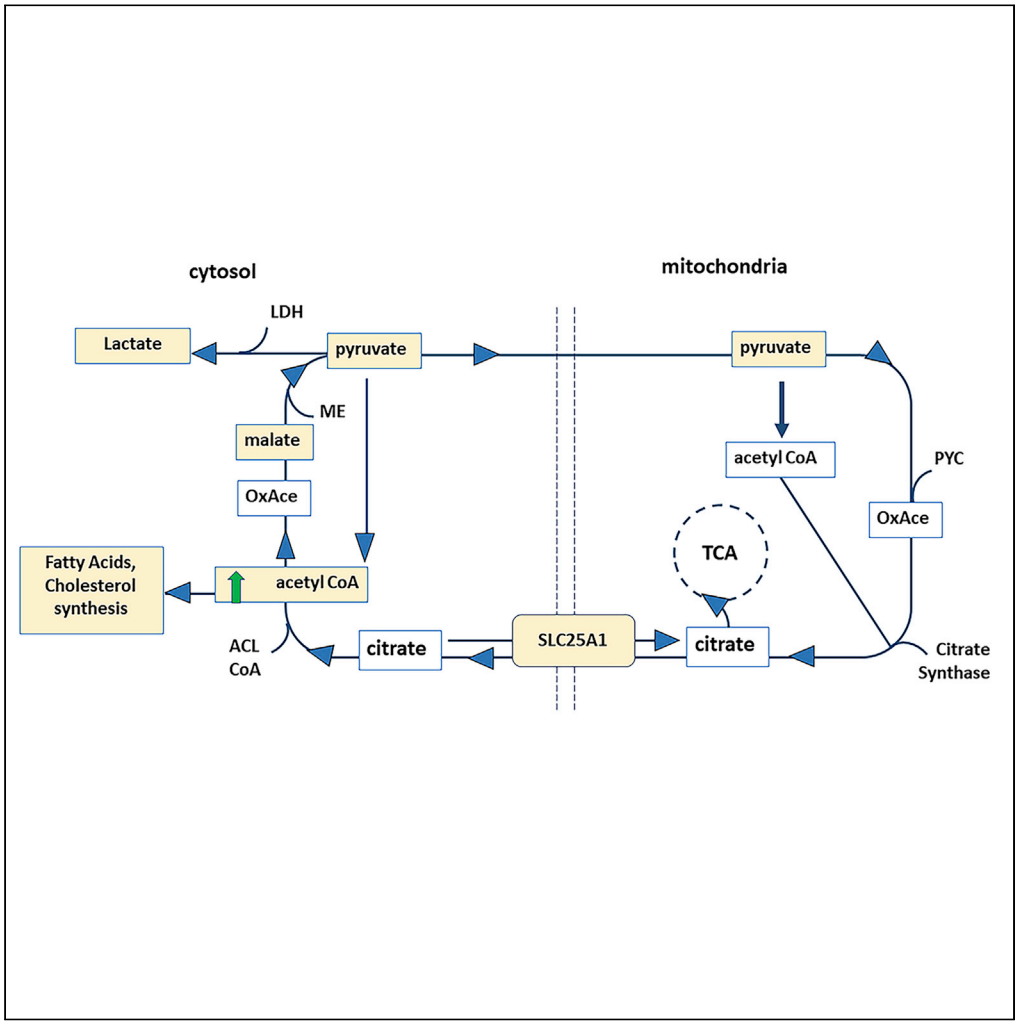

Kalimuthusamy Natarajaseenivasan, Alvaro Garcia, Prema Velusamy, Santhanam Shanmughapriya, Dianne Langford

dianne.langford@temple.edu

Highlights

Astrocyte-neuron metabolic coupling maintains brain lipid homeostasis

Neurons are highly sensitive to toxic peroxidated fatty acids (pFA)

Accumulation of pFA in neurons induces autophagy and release of pFA

Citrate shuttling in astrocytes is required to process excess neuron-derived pFA

Natarajaseenivasan et al., iScience 25, 105407 November 18, 2022
https://doi.org/10.1016/j.isci.2022.105407

iScience

CellPress
OPEN ACCESS

Article

Citrate shuttling in astrocytes is required for processing cocaine-induced neuron-derived excess peroxidated fatty acids

Kalimuthusamy Natarajaseenivasan,[1,2] Alvaro Garcia,[1] Prema Velusamy,[3] Santhanam Shanmughapriya,[3] and Dianne Langford[1,4,*]

SUMMARY

Disturbances in lipid metabolism in the CNS contribute to neurodegeneration and cognitive impairments. Through tight metabolic coupling, astrocytes provide energy to neurons by delivering lactate and cholesterol and by taking up and processing neuron-derived peroxidated fatty acids (pFA). Disruption of CNS lipid homeostasis is observed in people who use cocaine and in several neurodegenerative disorders, including HIV. The brain's main source of energy is aerobic glycolysis, but numerous studies report a switch to β-oxidation of FAs in response to cocaine. Unlike astrocytes, in response to cocaine, neurons cannot efficiently consume excess pFAs for energy. Accumulation of pFA in neurons induces autophagy and release of pFA. Astrocytes endocytose the pFA for oxidation as an energy source. Our data show that blocking mitochondrial/cytosolic citrate transport reduces the neurotrophic capacity of astrocytes, leading to decreased neuronal fitness.

INTRODUCTION

Pharmacologic and neuroimaging data report that cocaine use disrupts CNS energy metabolism, alters lipid content of the brain, and causes abnormal phospholipid metabolism and biosynthesis (Volkow, et al., 1990, Volkow, et al., 1993; Ross et al., 2002; Nogueiras et al., 2008; Volkow et al., 2010; Kovalevich et al., 2012a, 2012b; Boury-Jamot et al., 2016; Shao et al., 2019). Low cholesterol and FA levels in the blood of people addicted to cocaine are associated with relapse (Buydens-Branchey and Branchey 2003; Buydens-Branchey et al., 2003a; Buydens-Branchey et al., 2003b). In fact, extensive cocaine-induced changes in brain lipidomics in rodents contribute to addiction, supporting these findings in humans (Cummings et al., 2015; Bodzon-Kulakowska et al., 2017; Lin et al., 2017a, 2017b).

A recent systematic review discussed studies addressing proteomic and metabolic changes associated with neurocognitive function in people with HIV (PWH) and reported alterations in several proteins and metabolites related to neurochemical pathways (Williams et al., 2021). In the absence of substance use, including cocaine, progressive disturbances in brain lipidomics as assessed via cerebrospinal fluid (CSF) are reported that include abnormal cholesterol and sphingolipid metabolism (Haughey et al., 2004; Mielke et al., 2010; Bandaru et al., 2013). In other studies, disruptions in normal bioenergetic pathways were reported in the brains' of PWH, and data showed that bioenergetic disruptions correlated with viral RNA levels (Sanna et al., 2021); however, cocaine use was not considered.

Using cocaine increases the risk for HIV infection, and PWH who use cocaine have metabolic disturbances in the brain that contribute to the progression of HIV-associated neurocognitive disorders (HAND) (Purohit et al., 2011; Buch et al., 2012). Clinical studies in PWH and *in vitro* and *in vivo* research show that cocaine use exacerbates HIV impairment of metabolic processes at the cellular and whole-brain levels (Ernst et al., 2003; Ratai et al., 2011; Young et al., 2014; Dickens et al., 2015; Cotto et al., 2018b; Cotto et al., 2019; Deme et al., 2020). Moreover, cocaine has been linked to increased HIV replication, viral activation during latency, and disruption of innate immune responses (Tyagi et al., 2016). Despite these connections, little is known about how cocaine contributes to disruptions in lipid and FA utilization in chronic HIV infection of the brain or to viral dynamics in new infections.

[1]Department of Neural Sciences, Lewis Katz School of Medicine at Temple University, Philadelphia, PA, USA

[2]Department of Microbiology, Bharathidasan University, Tiruchirapalli, India

[3]Heart and Vascular Institute, Department of Medicine, Department of Cellular and Molecular Physiology, Pennsylvania State University, College of Medicine, Hershey, PA, USA

[4]Lead contact

*Correspondence: dianne.langford@temple.edu

https://doi.org/10.1016/j.isci.2022.105407

Astrocytes provide energetic support to neurons by direct metabolic coupling interactions that deliver lactate and cholesterol to neurons (Tsacopoulos and Magistretti 1996, Allaman et al., 2008). Lactate generated by astrocytes is taken up by neurons and is a key metabolite for neuronal aerobic metabolism to meet their high energetic demands (Bolanos et al., 2010; Suzuki et al., 2011). Our recent studies in human primary neurons and astrocytes and in mice show that cocaine and the HIV protein, Tat, decrease astrocyte neurotrophic support and impair lipid homeostasis. In astrocytes exposed to cocaine, pyruvate is diverted toward acetyl CoA production to the tricarboxylic acid cycle (TCA), bypassing conversion to lactate for neurons (Cotto et al., 2018b). Neurons have a robust aerobic metabolism; whereas astrocytes rely primarily on ATP generated from glycolysis (Dienel and Hertz 2001; Magistretti 2006, Bolanos et al., 2010; Suzuki et al., 2011). Astrocytes exposed to cocaine and Tat switch from glucose metabolism to fatty acid oxidation (FAO) by increasing mitochondrial β-oxidation to generate more ATP (Natarajaseenivasan et al., 2018). In addition, astrocytes synthesize apolipoprotein E (ApoE) to shuttle lipids to neurons through the ATP-binding cassette transporter, ABCa1 (Hirsch-Reinshagen et al., 2004; Yassine et al., 2016). Exposure of astrocytes to cocaine and Tat decreases ApoE and ABCa1 levels and reduces biosynthesis of cholesterol and its transfer to neurons (Cotto et al., 2018b).

Normally, this system is tightly regulated, but during challenges by cocaine or with HIV infection, astrocytes respond by increasing their metabolism, which is energetically expensive and changes their mitochondrial bioenergetics (Buch et al., 2012; Cisneros et al., 2018; Cotto et al., 2018b; Natarajaseenivasan et al., 2018). For example, we showed that astrocytes exposed to cocaine and Tat switch from glucose metabolism to β-oxidation (Natarajaseenivasan et al., 2018). On the other hand, neurons exposed to cocaine or Tat generate excess toxic peroxidated fatty acids (pFA) due to increased ROS (Ioannou et al., 2019), induce autophagy, quickly quench their antioxidant capacity, and expel pFA. Astrocytes take up pFA from neurons for processing and for use as an energy source (Barber and Raben 2019). Thus, disrupted lipid metabolic coupling between astrocytes and neurons exposed to cocaine/Tat leads to homeostatic imbalance.

Data from previous studies provide information regarding key links in the signaling pathways likely involved in cocaine- and HIV-mediated CNS lipid metabolic disruptions.

Pyruvate is a rate-limiting factor in lactate production and acetyl-CoA for cholesterol and ATP synthesis. Thus, directing pyruvate toward lactate production and acetyl-CoA toward cholesterol synthesis would increase astrocyte-derived neurotrophic support. Through lipolysis, neuron-derived fatty acids (FA) are taken up by astrocytes and delivered to mitochondria for use as an alternative energy source. Astrocytes respond to the uptake of pFA by upregulating genes for energy metabolism and oxidative species neutralization and by enhancing the metabolism of lipid droplets (LD) via mitochondrial β-oxidation (Bailey et al., 2015; Liu et al., 2015; Ioannou et al., 2018). The increased uptake and processing of pFA by astrocytes shifts them asway from their neurotrophic capacity as shown by decreased cholesterol and lactate production, which can lead to neuronal dysfunction (Natarajaseenivasan et al., 2018). Citrate shuttles between the cytoplasm and mitochondria via the citrate carrier, SLC25A1, that is responsible for balancing citrate levels in both compartments (Mosaoa et al., 2021). SLC25A1 transports citrate between the mitochondria and cytosol, thereby regulating citrate levels within the cell and significantly influencing acetyl-CoA and pyruvate availability. Cytosolic citrate is a precursor for acetyl-CoA leading to cholesterol and FA synthesis (Fernandez et al., 2018; Mosaoa et al., 2021). Mitochondrial citrate stimulates the TCA cycle and promotes oxidative phosphorylation.

The HIV-1 transactivator protein, Tat, is a viral protein that activates viral transcription. Independently of its transcriptional activity, Tat induces oxidative stress, mitochondrial dysfunction, and metabolic disturbances in the brain (Sivalingam et al., 2021). Importantly, Tat is not eliminated in HIV-infected individuals on cART, and even in the absence of productive viral replication, a significant amount of Tat is produced (Bayer et al., 1995; Westendorp et al., 1995; Xiao et al., 2000; Marcondes et al., 2001; Nath 2002; Jaeger and Nath 2012).

Based on our previous data, it is likely that cocaine and Tat will impact the flux of mitochondrial and cytosolic citrate in astrocytes given the switch in β-oxidation (Natarajaseenivasan et al., 2018). Disruptions in SLC25A1 functioning are linked to at least 11 different CNS diseases characterized by defective lipid utilization and mitochondrial energy production (Infantino et al., 2007; Palmieri 2013, Di Noia et al., 2014; Donadelli et al., 2014; Giangregorio et al., 2014; Infantino et al., 2014). Once in the cytosol, citrate is converted to acetyl CoA and oxaloacetate, ultimately leading to cholesterol and lactate synthesis, respectively both of

which may be transported to neurons. Despite an extensive literature showing that cocaine and HIV disrupt astrocyte/neuron lipid exchange, there is currently a gap in our knowledge regarding the effects of cocaine and HIV on astrocyte FA utilization and the impact that these changes have on neuronal fitness and survival. The current study will examine the combined impact of cocaine and HIV on impaired metabolic function by investigating how astrocyte-neuron metabolic coupling maintains brain lipid homeostasis during exposure to the HIV protein, Tat, and cocaine. We also address how neurons that are highly sensitive to toxic pFA accumulate pFA and roles that autophagy release of pFA play in neuronal survival during stress. Finally, we show the uptake of pFA by astrocytes and the importance of citrate shuttling to process excess neuron-derived pFA.

RESULTS

Cocaine and Tat increase mitochondrial reactive oxygen species in neurons

To determine if exposure to cocaine and/or the HIV protein, Tat, triggers peroxidation of FA in neurons, we exposed neurons to HIV-1 MN Tat (50 ng/mL), cocaine (5μM), or both every 24 h for 48 h, as previously reported (Kovalevich, 2012a; Kovalevich et al., 2012b; Kovalevich, 2015; Cotto et al., 2018b; Mohseni Ahooyi T et al., 2018; Natarajaseenivasan et al., 2018). Previous studies report that cocaine and Tat alter NMDAR subunit composition, synaptic redistribution, and changes in protein levels, leading to activation of neuronal NMDA signaling and excitotoxicity (Ortinski 2014; Hu 2016). Thus, neurons treated 4 h with 500nm NMDA were used as a control, and the lipid soluble antioxidant, α-tocopherol (50 μM), was used to block lipid peroxidation (Ioannou et al., 2019). Rhodamine 123 was used to label active mitochondria, and MitoSOX red detects mitochondria-derived reactive oxygen species (ROS). Results show that cocaine and Tat, alone or in combination, induce significant levels of mitochondrial ROS compared with untreated neurons (Figures 1A and 1B). However, no additive or synergistic effects were observed in cocaine- + Tat-treated neurons. As expected, α-tocopherol blocked cocaine-, Tat-, and NMDA-induced mitochondrial ROS formation.

Accumulation of peroxidated lipids induces autophagy and release of lipids from neurons

Neurons do not typically form significant numbers of LD (Schonfeld and Reiser 2013, Ioannou et al., 2019). However, during stressful conditions including inflammation, increased levels of ROS, or in the presence of aberrant proteins in neurodegeneration, neurons accumulate FA into LD (Pennetta and Welte 2018, Ioannou et al., 2019; Farmer et al., 2020). In this context, our data show that cocaine and Tat increased neuronal mitochondrial ROS (Figure 1) and accumulation of lipids and pFA (Figure 2). As expected, BODIPY 493/503-labeled neurons exposed to cocaine, Tat, or both showed significantly increased levels of LD ($p < 0.001$) compared with untreated control neurons (red) (Figures 2A and 2B); however, α-tocopherol prevented accumulation of LD. In agreement with previous data (Ioannou et al., 2019), a significant fraction of total lipids in neurons exposed to cocaine and Tat were peroxidated as determined by the lipid peroxidation sensor assay (BD-C11, green), with cocaine driving greater ratios of peroxidation ($p < 0.001$) compared with Tat ($p < 0.05$) (Figures 2C and 2D). Given that neurons have limited capacity to quench peroxidated lipids, autophagy may be induced to remove toxic lipids, as previously reported (Ioannou et al., 2019). To assess if accumulation of pFA triggered autophagic pathways, changes in levels of the autophagy markers, LC3B-I and II, ratios, and pAMPK were measured in neurons exposed to cocaine, Tat, or NMDA. LC3B-I levels were significantly decreased in neurons exposed to cocaine and Tat ($p < 0.01$), whereas LC3B-II was significantly increased ($p < 0.01$), suggesting that LC3B-I was converted to LC3B-II (Figures 3A–3D). These changes in LC3BI/II and ratios in response to Coc/Tat were prevented by the presence of α-tocopherol. Increased levels of phosphorylated AMPK ($p < 0.01$) in response to cocaine and Tat accompanied these changes (Figure 3E), but once again α-tocopherol blocked phosphorylation of AMPK.

Neurons exposed to Tat, cocaine, Tat + cocaine, or NMDA with and without α-tocopherol were cultured with BODIPY 558/568 to label lipids (Figure S1). Flow cytometric analyses of cell-free media containing fluorescently labeled lipids indicated that Tat alone and in combination with cocaine increased the numbers of lipids present in the media as well as intensity of labeling (Figures S1A–S1D and S1F). NMDA used as a positive control (Figures S1E and S1F) showed similar profiles to Tat, cocaine, and Tat + cocaine (Figures S1B–S1D and S1F).

Peroxidated lipids are transferred from neurons to astrocytes for FAO

Accumulation (Figure 2) and release (Figures 3 and S1) of pFA by neurons exposed to Tat, cocaine, or NMDA (Ioannou et al., 2019) are predicted to be accompanied by uptake and processing of FA by

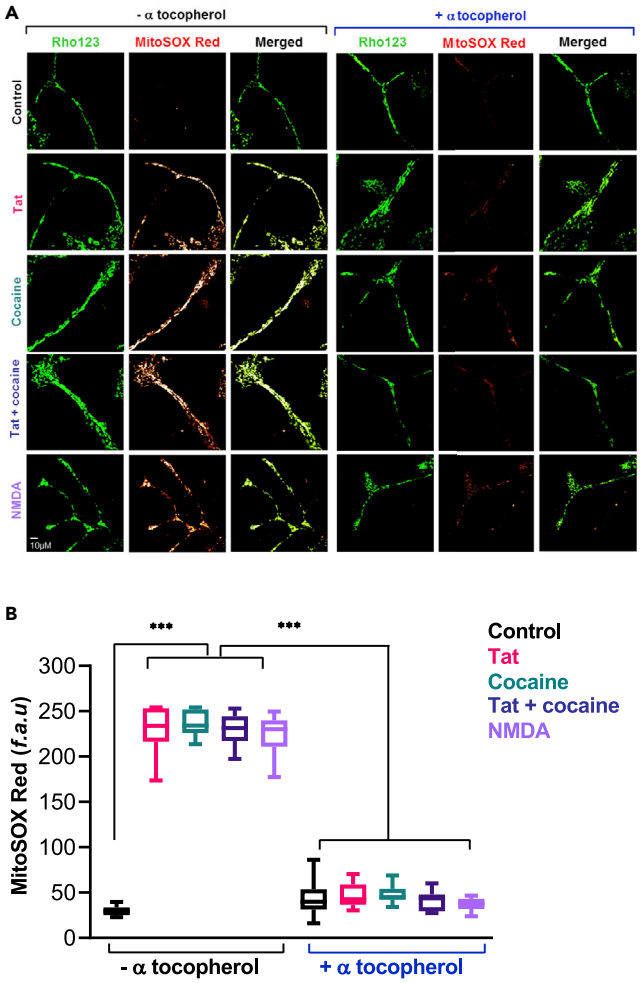

Figure 1. Tat and cocaine exposure induces mitochondrial reactive oxygen species production (mROS) in neurons

Human primary neurons exposed to Tat (50 ng/mL), cocaine (5 μM), both Tat and cocaine, or NMDA (100 μM) either in the presence or in the absence of α-tocopherol (50 μM) were labeled with the mROS indicator, MitoSOX.

(A and B) Representative confocal images of neurons labeled with MitoSOX red and (B) quantification of MitoSOX fluorescence intensity. Increased mROS generation was detected in neurons exposed to Tat, cocaine, or NMDA; however, treatment with α-tocopherol (an ROS quencher) quenched mROS generation. Neurons with no exposure to Tat, cocaine, or NMDA were used as control. ***p<0.001.

astrocytes. To confirm uptake of FA by astrocytes, neurons were cultured with BODIPY 558/568 for lipid labeling (red) with and without cocaine, Tat, or both, and astrocytes were cultured with rhodamine 123 to label mitochondria (green). Cell-free neuronal conditioned media (NCM) was collected and placed onto astrocytes +/− α-tocopherol. Unlike astrocytes exposed to NCM from untreated neurons, astrocytes exposed to media from neurons treated with Tat, cocaine, both, or NMDA showed significantly greater uptake of neuron-derived lipids (red) (Figures 4A and 4B) ($p < 0.001$). In fact, perilipin, an LD protein that protects LD from autophagy, was increased significantly in astrocytes fed LDs from neurons exposed to cocaine and Tat (data not shown). Because autophagy can be induced in situations of increased LD packaging of lipids as a means for cell survival, our observation that autophagy was increased in neurons requires further investigation.

Citrate shuttling in astrocytes is required to process cocaine-induced neuron-derived excess peroxidated fatty acids

Previous studies report that astrocytes are the main source of citrate in the CNS (Westergaard et al., 2017). Our previous data show that upon exposure to cocaine or Tat, astrocytes switch from

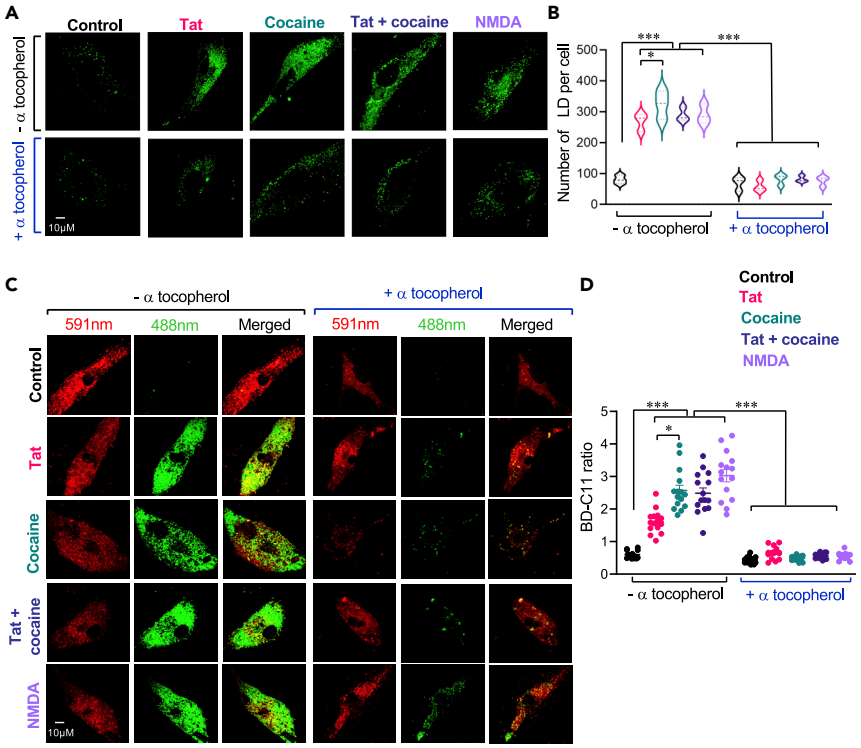

Figure 2. Tat and cocaine exposure results in lipid accumulation and fatty acid peroxidation in neurons

Control or N2A neurons exposed to Tat (50 ng/mL) and/or cocaine (5 μM) or NMDA (100 μM) either in the presence or in the absence of α-tocopherol (50 μM) (an ROS quencher) were labeled with BODIPY 493/503 (green) for total lipids (1 μM) (A and B) or BD-C11 for peroxidated lipids (C and D), and accumulation of lipids was measured using confocal microscopy.

(A and B) Representative confocal images of neurons labeled with BODIPY 493/503 (green) to show total lipids and (B) quantification of the number of lipids/cell showing increased accumulation of lipids in neurons exposed to Tat, cocaine, and NMDA. Treatment with tocopherol prevented lipid accumulation.

(C) Representative confocal images of neurons labeled with BODIPY C11 for unperoxidated lipids (red) and the shift to peroxidated lipids (green).

(D) Quantification of BD-C11 ratio (green to red) in neurons shows increased peroxidation of lipids in Tat-, cocaine-, and NMDA-treated neurons. Treatment with α-tocopherol prevented lipid peroxidation. Data indicate Mean ± SEM; ***p < 0.001, **p < 0.01, *p < 0.05; n = 3 coverslips with analyses of 5 cells per coverslip for all experiments.

glucose to FA oxidation (Natarajaseenivasan et al., 2018). Given that SLC25A1 transports citrate from the cytosol into the mitochondria for entrance into the TCA cycle, we reasoned that loss of citrate transport in response to increased pFA uptake would impact β-oxidation. To assess the importance of citrate shuttling in the processing of neuron-derived pFA, SLC25A1 was knocked down (KD) in astrocytes, and cells were then exposed to neuron-conditioned media (NCM) from untreated neurons or neurons exposed to cocaine, Tat, or both. Western analyses confirm KD of SCL25A1 (Figures 5A and 5B). Astrocytes were cultured in the presence of BODIPY 493/503 (green) with SCL25A1 KD or Scr siRNA and exposed to NCM (Figure 5C). In SLC25A1 KD astrocytes, significantly increased accumulation of lipids was observed compared with astrocytes with scrambled siRNA (Figures 5C and 5D), suggesting decreased lipid processing. Our previous studies showed that exposure of astrocytes directly to cocaine and Tat decreased the cholesterol synthesis (Cotto et al., 2018b). Normal levels of cholesterol in astrocytes triggers LXR activation, leading to the transcription of target genes involved in cholesterol trafficking and efflux, including ApoE, SREBP, and several ATP-binding cassette transporter proteins, including ABCa1 (Cotto et al., 2018b). Knockdown of SLC25A1 in astrocytes treated with NCM from neurons exposed to Tat, cocaine, or both had decreased intracellular and extracellular cholesterol (Figures 5F and 5G) as well as lower levels of ApoE (Figure 5H). These data support the importance of citrate shuttling to maintain lipid processing and normal cholesterol levels.

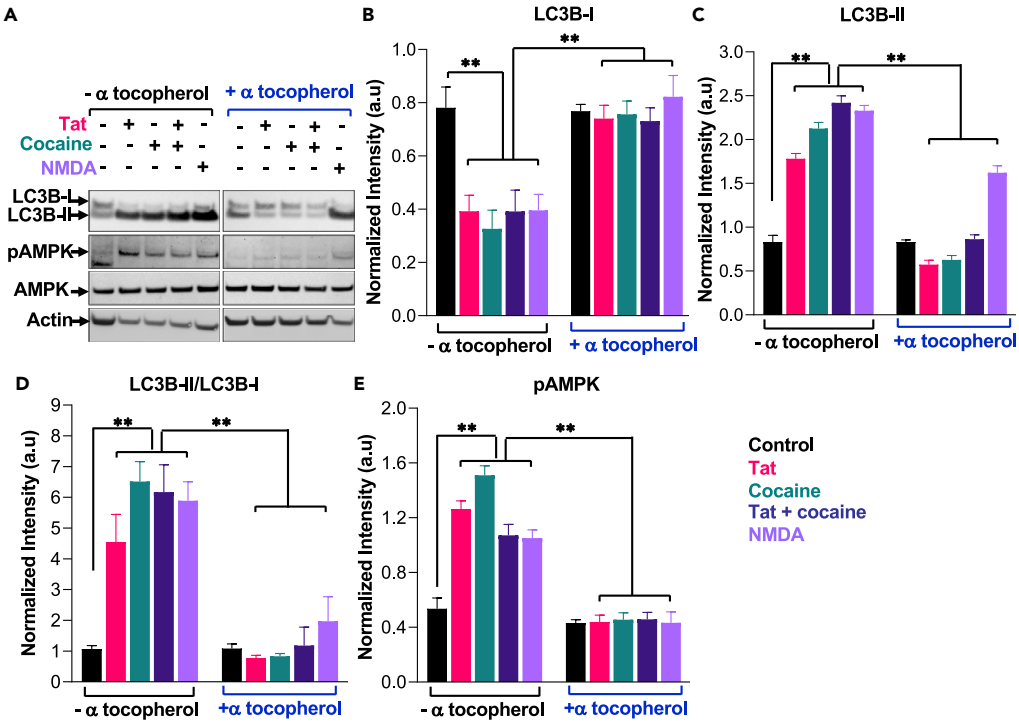

Figure 3. Accumulation of peroxidated lipids induces autophagy in human neurons

Control or neurons exposed to Tat (50 ng/mL) and/or cocaine (5 mM) or NMDA (100 mM) either in the presence or in the absence of α-tocopherol (50 mM) (an ROS quencher) were western blotted for the autophagy markers LC3B and pAMPK. (A–E) Representative western blot and (B–D) quantification of the normalized LC3B-I (B), LC3B-II (C), LC3B-I/LC3B-II ratios (D), and pAMPK (E) protein levels indicate increased autophagy in neurons exposed to Tat/cocaine/NMDA. Data indicate Mean ± SEM; ***p < 0.001, **p < 0.01, *p < 0.05; n = 3 independent experiments.

Citrate shuttling is important for mitochondrial respiration in astrocytes during neuronal challenge with Tat and cocaine

Our previous data also show that direct exposure of astrocytes to Tat and cocaine induces a switch in astrocyte metabolism from glucose to fatty acid oxidation (Natarajaseenivasan et al., 2018). To investigate if bioenergetic disruptions were observed in astrocytes exposed to NCM from untreated neurons or neurons exposed to cocaine, Tat, or both in the presence or absence of SCL25A1, mitochondrial oxygen consumption rates were assessed. Supplementary data show that neurons exposed to Tat, cocaine, or both where palmitate was used as an FA substrate showed minimal response to oligomycin, FCCC, or rotenone (Figure S2). In fact, in cocaine- and in Tat + cocaine-treated neurons, basal oxygen consumption rate (OCR), maximal OCR, and ATP couple respiration were significantly decreased ($p < 0.001$) compared with untreated and Tat-treated neurons (Figures S2A–S2D). On the other hand, basal OCR, maximal OCR, and ATP production were increased significantly in astrocytes treated with media from neurons exposed to Tat, cocaine, or both (Figures S2E–S2G), with no change in nonmitochondrial respiration (Figure S2H), and as previously reported (Natarajaseenivasan et al., 2018). Palmitate was used as the substrate for FAO, and BSA was used as the non-FA substrate. The FAO inhibitor, etomoxir, blocked FAO production in the presence of palmitate.

As predicted, basal and maximal oxygen consumption rates and ATP-coupled respiration were increased in astrocytes exposed to NCM from Tat-/Coc-treated neurons (Figures 6A and 6C–6E). On the other hand, blocking citrate transport by KD SLC25A1 (Figure 6B) prevented increased basal and maximal oxygen consumption rates and ATP-coupled respiration induced by exposure of astrocytes to NCM from Tat-/Coc-treated neurons (Figures 6C–6E) in astrocytes. Nonmitochondrial respiration was not affected by NCM or SCL25A1 KD in any conditions (Figure 6F). These data support an important role for citrate shuttling in mitochondrial respiration during neuronal challenge with Tat and cocaine.

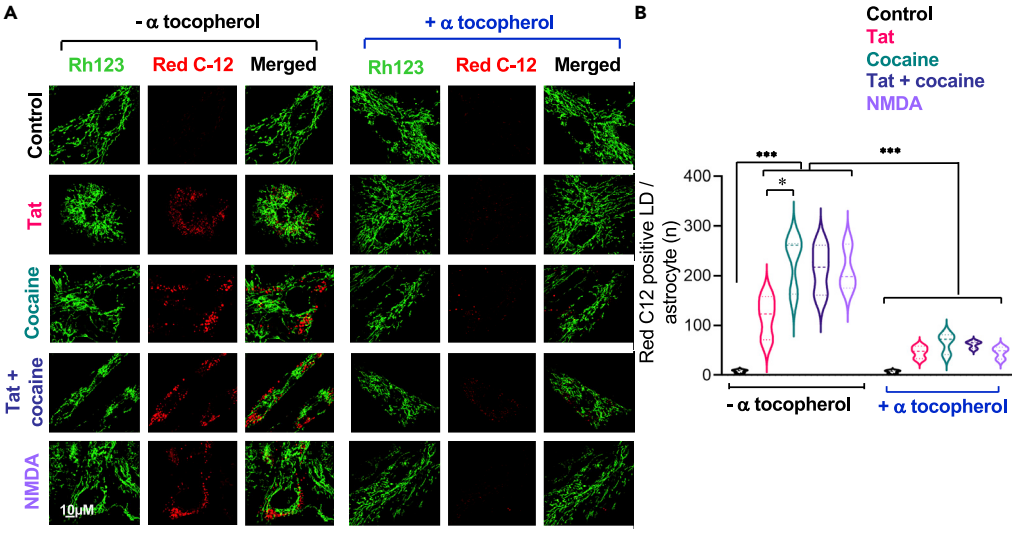

Figure 4. Cocaine and/or Tat exposure facilitates transfer of lipids from neurons to astrocytes

Control rat neurons or neurons exposed to Tat (50 ng/mL) and/or cocaine (5 μM) or NMDA (100 μM) in the presence or absence of α-tocopherol (50 μM) (an ROS quencher) were cultured with BODIPY 558/568 (1 mM) for lipid labeling. After incubation, the cell-free neuronal media was collected and rat astrocytes were cultured with this media for 16 h. The transfer of lipid droplets from neurons to astrocytes was observed by confocal microscopy. The astrocyte mitochondria were stained with rhodamine 123 (488 nm), and lipid droplets from neurons were stained red (561 nm).

(A and B) Representative confocal images of astrocytes treated with neuronal-conditioned media and (B) quantification of the number of red C-12 positive lipid droplets per astrocyte (LD/astrocyte) showing increased transfer of lipids from neurons exposed to Tat, cocaine, or NMDA to astrocytes. Media from α-tocopherol-treated neurons with or without exposure to Tat, cocaine, or NMDA showed no lipid transfer. Data indicate Mean ± SEM; ***$p < 0.001$; $n = 3$ independent coverslips and 5 cells/coverslip were analyzed. *$p<0.05$.

Knocking down SLC25A1 limits the neurotrophic capacity of astrocytes

To further assess the potential importance of citrate shuttling in astrocytes challenged with processing neuron-derived pFA, SLC25A1 was knocked down (KD) in astrocytes; we utilized a transwell culture system. Astrocytes were plated onto the upper chamber of a transwell, and untreated neurons were plated onto the well below in the lower chamber. In a separate experiment, NCM was collected from untreated neurons or neurons exposed to cocaine, Tat, or both. NCM containing neuron-derived LD/pFA (as shown in Figure S1) was then placed onto astrocytes cultured in the upper transwell chamber. After 24 h in co-culture with astrocytes, neurons were collected from the bottom chamber for analyses of neuronal fitness (Figures 7A, 7D, and 7E) and survival (Figure 7F). More efficient processing of pFA by astrocytes with functioning SLC25A1 provided neuronal protection as indicated by decreased levels of PSD95, MAP2, and ATP (Figures 7C–7E), whereas, without SLC25A1, astrocyte neurotrophic capacity was diminished as indicated by decreased levels of the post-synaptic marker PSD95, the dendritic marker MAP2, and ATP production.

Astrocytes were then assessed for intracellular and extracellular lactate levels, LDH activity, ATP production, and viability. Lactate levels and LDH activity were not altered in astrocytes treated with NCM, regardless of the presence or absence of SLC25A1 (Figures S3A–S3C); however, ATP levels were significantly decreased in astrocytes where SLC25A1 was KD (Figure S3D).

DISCUSSION

Tight metabolic coupling between neurons and astrocytes is critical for the overall health of the brain. Although neurons expend a considerable amount of ATP on neurotransmission, astrocytes provide neurons with metabolic substrates and antioxidants (Belanger and Magistretti 2009; Belanger et al., 2011). This metabolic support allows neurons to allocate more cellular resources to sustaining high activity rates during information processing (Farese and Walther 2009; Guo et al., 2009; Walther and Farese 2009). An important area in neuron-astrocyte interactions relates to the metabolism of FAs. FAs are components of phospholipids in cellular membranes and are stored within cells as energy-rich triacylglycerides localized

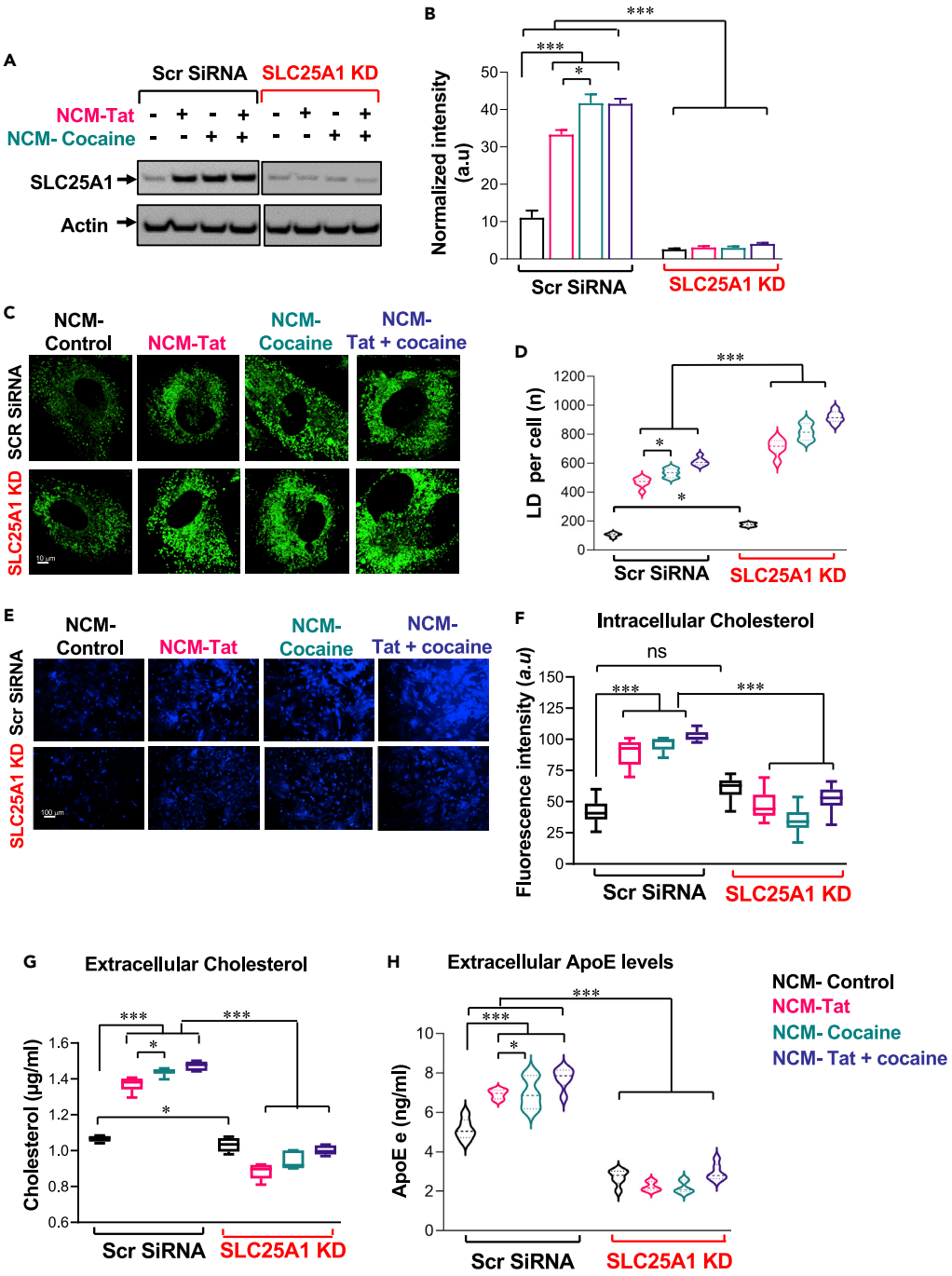

Figure 5. Conditioned media from Tat- and/or cocaine-treated neurons alters astrocytic cholesterol homeostasis

SLC25A1 was knocked down (KD) in rat astrocytes, and nontargeting scrambled siRNA (Scr siRNA) was used as a control. Astrocytes were then cultured with cell-free rat neuronal media (NCM) collected from either untreated or control or neurons exposed to Tat and/or cocaine. (A–D) Protein levels were assessed by western analyses for SLC25A1.

(A) Representative western blot and

(B) and quantification of the protein abundance SLC25A1 KD astrocytes.

(C and D) Astrocytes with SCL25A1 knocked down and cultured in the presence of BODIPY 493/503 (green) to label lipids show increased lipid accumulation compared with Scr siRNA upon exposure to Tat/cocaine NCM.

(E and F) Scr siRNA and SLC25A1 KD astrocytes treated with control or Tat/cocaine NCM were stained with Filipin III (blue) to visualize the intracellular cholesterol levels. Representative fluorescence microscopy images (E) and quantification of

Figure 5. *Continued*
Filipin fluorescence (F) show decreased accumulation of cholesterol in KD SCL25A1 astrocytes exposed to Tat and/or cocaine NCM.
(G and H) Extracellular cholesterol and ApoE protein levels were quantified in astrocyte media using ApoE ELISA and Amplex Red cholesterol assay, respectively. Astrocytes exposed to Tat and/or cocaine NCM show increased levels of cholesterol and ApoE, but knocking down SLC25A1 reduced cholesterol and ApoE levels. Data indicate Mean ± SEM; ***$p < 0.001$, *$p < 0.05$; 3 independent coverslips with 15–20 cells/coverslip analyzed.

to LDs. Under normal conditions, LDs are mostly found in liver and adipose tissues, and activity responds to changes in cellular signaling. Cells other than adipocytes, including neurons, can form LDs in response to cellular inflammations and stress (Teixeira et al., 2021). Evidence from multiple studies report the accumulation of LDs in the brain during normal aging, as well as in conditions of increased oxidative stress and inflammation (Meng et al., 2015; Shimabukuro et al., 2016; Kwon et al., 2017; Liu, 2017a, 2017b; Islam et al., 2019; Marschallinger and al., 2020) and in several neurodegenerative diseases, including amyotrophic lateral sclerosis, Huntington, Parkinson, and Alzheimer diseases (Farmer et al., 2020). In addition, changes in cholesterol and FA levels in the blood of people addicted to cocaine are associated with relapse (Buydens-Branchey and Branchey 2003; Buydens-Branchey et al., 2003a; Buydens-Branchey et al., 2003b).

Although this manuscript focuses on astrocyte-neuron metabolic coupling, the contributions of microglia to the regulation of lipid processing during stressful conditions of energy deficit should be considered. Healthy microglia clear lipids via cell surface scavenger receptors; however, aged or pro-inflammatory microglia accumulate cholesterol and other neutral lipids. In fact, our previous studies have shown that cocaine self-administration in rats increases microglial activation and that microglial-derived methyl-CpG-binding protein 2 (MeCP2) is a sensitive target of cocaine (Cotto et al., 2018a). MeCP2 negatively regulates the expression of brain-derived neurotrophic factor (BDNF). In the presence of cocaine, MeCP2 dissociates from the BDNF promoter, resulting in increased release of BDNF release, which may contribute to cocaine-induced synaptic plasticity. In the context of metabolic reprogramming and lipid processing during disease, evidence for microglial contributions in Alzheimer disease, multiple sclerosis, and schizophrenia is reported (Loving and Bruce 2020). Increased microglial expression of genes involved in lipid and lipoprotein metabolism including ApoE and lipoprotein lipase point to a role for microglia in neurodegenerative disease (Keren-Shaul et al., 2017). Studies in animal models addressing effects of both chronic HIV infection and cocaine use on brain metabolic reprogramming are needed to understand how all cellular components affect lipid production and processing. Investigations are currently underway in the Eco-HIV mouse with and without chronic cocaine administration to assess changes in CNS bioenergetics at global, cellular, and molecular levels.

Studies show that periods of high neuronal stress induce peroxidation of FAs and formation of LDs in neurons due to ROS triggering c-Jun-N-terminal kinase (JNK) and sterol regulatory-binding protein (SREBP) activity, followed by accumulation of LDs in astrocytes (Bailey et al., 2015; Liu et al., 2015). Because neurons have a low capacity for FA consumption in mitochondria, pFAs become toxic and must be expelled (Schonfeld and Reiser 2013, Sultana et al., 2013). In contrast to neurons, astrocytes store energy in the form of LDs and can effectively manage oxidative stress (Belanger and Magistretti 2009, Belanger et al., 2011), suggesting that the transfer of pFAs from neurons to astrocytes may benefit both cell types. In fact, Ioannou et al., demonstrated that stressed neurons expel toxic FAs in association with ApoE-positive lipid particles and that nearby astrocytes endocytose these LDs (Ioannou et al., 2018, Ioannou et al., 2019). In astrocytes, the LDs are broken down, and liberated FAs are fed into the mitochondria as fuel for oxidative phosphorylation (Ioannou et al., 2019). In this context, our studies sought to determine whether cocaine and HIV contribute to neuronal-pFA accumulation and uptake by astrocytes as a result of astrocyte-neuron lipid metabolic crosstalk. Our data show that cocaine and the HIV protein, Tat, increase the accumulation and release of pFA from neurons. In turn, we show that astrocytes take up the pFAs expelled by neurons and increase FA-dependent oxygen consumption rate and ATP production. Importantly, this was not observed in astrocytes exposed to cocaine and/or Tat. In addition to transfer of pFA from neurons to astrocytes as a means to manage oxidative stress, autophagy as well plays an important role in neuronal oxidative stress relief. In fact, because lipid metabolism is involved in the formation of autophagic membranes during stress (Xie et al., 2020), understanding the potential contribution of changes observed in neuronal pFA accumulation, processing, and expulsion requires consideration of autophagy as a means to degrade pFAs. Because autophagy can be induced in situations of increased LD formation as a means for cell survival, our observation that autophagy was increased in neurons requires further investigation. On

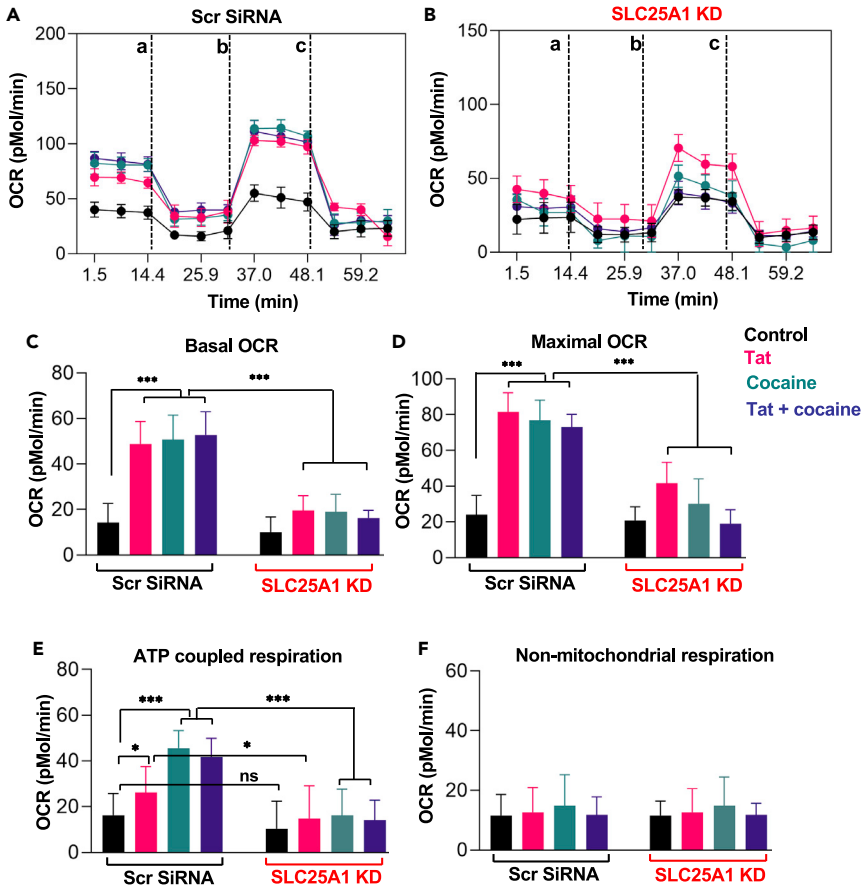

Figure 6. Citrate shuttling is important for mitochondrial respiration in astrocytes during neuronal challenge with Tat and cocaine

Rat astrocytes transfected with siRNAs against SLC25A1 or control nontargeting/scrambled siRNA (Scr siRNA) were cultured with cell-free neuronal-conditioned media (NCM) collected from untreated neurons or neurons exposed to Tat (50 ng/mL) and/or cocaine (5 μM).

(A and B) Mean traces of oxygen consumption rate (OCR) in astrocytes using palmitate as a substrate and after sequential exposure to oligomycin (a), FCCP (b), and rotenone/antimycin (c) shows reduced fatty acid oxidation (FAO) in astrocytes where SLC25A1 is knocked down.

(C–F) Quantification of basal OCR, (D) maximal OCR, (E) ATP-coupled respiration, and (F) nonmitochondrial respiration. Data indicate Mean ± SEM; ***p < 0.001, **p < 0.01, *p < 0.05; n = 24 independent wells of a 96 well plate.

the other hand, perilipin, an LD protein that protects LD from autophagy, was increased significantly in astrocytes fed LDs from neurons exposed to cocaine and Tat (data not shown), further supporting addition studies into the role versus autophagy in neuron versus astrocyte response to cocaine and Tat.

In this context, pyruvate is the rate-limiting factor in the production of lactate and acetyl Co-A for FA, cholesterol, and ATP synthesis. To maintain sufficient levels of metabolic substrates in the cytosol and mitochondria, the SCL25A1 transporter shuttles citrate from the mitochondria and vice versa. Citrate is converted back to acetyl CoA that can then be used for FA synthesis. In the mitochondria, acetyl CoA + oxaloacetic acid is catalyzed into citrate that then enters the TCA cycle for ATP production. Thus, SLC25A1 is required for citrate transport, oxidative phosphorylation, and FA oxidation. Our data confirmed the importance of citrate transport for astrocytes to maintain a neurotrophic phenotype in the presence of cocaine and Tat.

Data show that CNS metabolic disturbances observed in PWH and in cocaine users are exacerbated in PWH who use cocaine. Disruption of this tightly coordinated coupling to metabolize FAs likely contributes to the increased astrocytic energy metabolism and neuronal energy deficit reported during detrimental synergy between HIV infection and cocaine use.

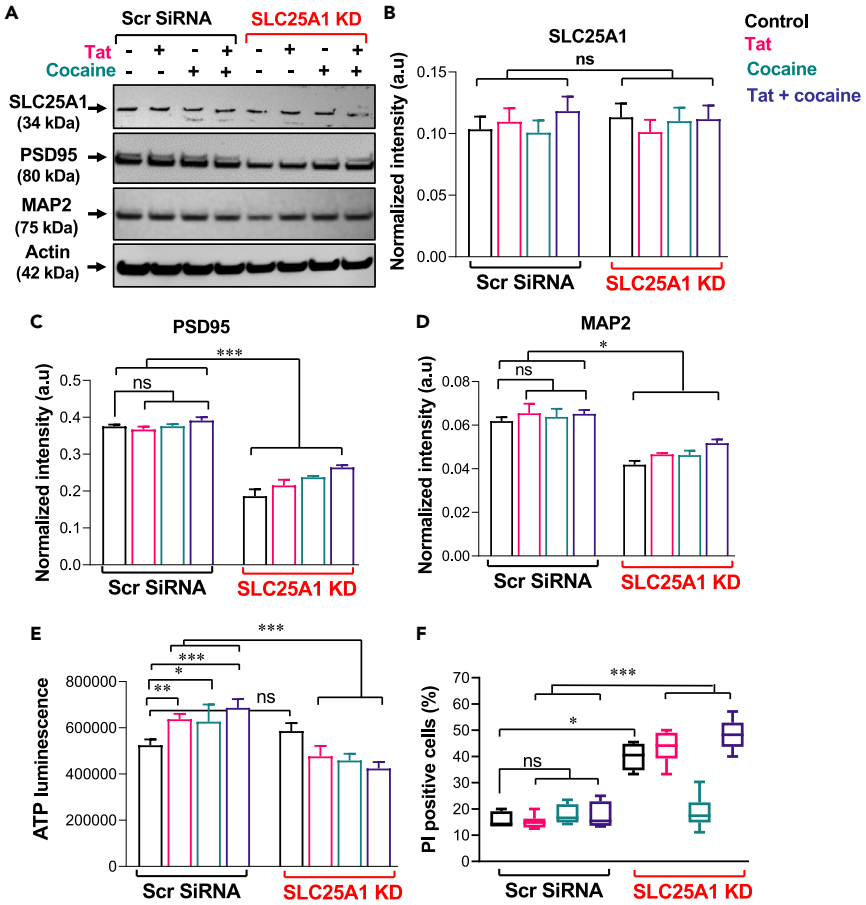

Figure 7. Knocking down SLC25A1 limits the neurotrophic capacity of astrocytes and decreases neuronal viability

Rat astrocytes and neurons were co-cultured using a transwell system. SLC25A1 was KD in astrocytes nontargeting/scrambled siRNA (Scr siRNA) as a control. Astrocytes were cultured on the upper chamber of a transwell. Neurons were plated onto the wells below and were untreated or exposed to cocaine, Tat, or both. Neuronal-conditioned media (NCM) was added to the upper chambers containing astrocytes, and after 24 h, neurons were collected from the bottom chamber for analyses.

(A–E) Representative western blot of neuronal lysates with antibodies against

(B) SLC25A1, (C) PSD95, and (D) MAP2 shows decreased neuronal markers and (E) less ATP production in the absence of SLC25A1.

(F) Neurons were stained with Hoechst (5 μg/mL) and propidium iodide (PI, 1 μg/mL) and cell death was assessed by confocal microscopy. Neurons co-cultured with SLC25A1 KD astrocytes show an increased % of PI positive cells. Data indicate Mean ± SEM; ***p < 0.001, **p < 0.01, *p < 0.05; n = 6 independent experiments with quantification of at least 10 fields/condition from each replicate.

We sought to determine how cocaine and HIV contribute to uncoupling of astrocyte-neuron metabolic crosstalk. Our data show that cocaine and the HIV protein, Tat, increase the accumulation and release of pFA from neurons. In turn, we show that astrocytes take up the pFA expelled by neurons and increased oxygen consumption rate and ATP production.

Pyruvate is a rate-limiting factor in the production of lactate and acetyl CoA for fatty acid, cholesterol, and ATP synthesis (Graphical Abstract). To maintain sufficient levels of metabolic substrates in the cytosol and the mitochondria, the SCL25A1 transporter carries citrate from the mitochondria into the cytosol and vice versa. Citrate is converted back to acetyl CoA that can be utilized for FA synthesis. In the mitochondria, acetyl CoA + oxaloacetic acid is catalyzed into citrate that then enters into the TCA cycle for ATP production. The citrate carrier, SLC25A1, is required for citrate transport oxidative phosphorylation and FAO. In the cases of cocaine and Tat in astrocytes, conversion of pyruvate to acetyl CoA and oxygen consumption

rate and ATP production increase significantly, thereby utilizing mitochondrial citrate for oxidation rather than FA acid production in the cytosol. Our data showed the importance of citrate transport for astrocytes to maintain a neurotrophic phenotype in the presence of cocaine or Tat.

Previous studies report that cocaine and Tat alter NMDAR subunit composition, synaptic redistribution, and changes in protein levels, leading to activation of neuronal NMDA signaling and excitotoxicity (Ortinski 2014; Hu 2016). Cocaine appears to drive the generation of pFA generation and autophagy in neurons; whereas, in astrocytes treated with neuron-conditioned medium, cocaine drives lipid droplet formation and uptake of neuron-derived lipids, ATP-coupled respiration, and increased expression of SLC25A1. Tat, on the other hand, in general had less impact on lipid metabolism than cocaine. Likewise, little to no additive effects were observed with cocaine and Tat together. Of note, the choice of Tat from among the HIV components was based upon its well-established stimulation of inflammatory cytokine and ROS production, induction of cytotoxicity, and presumed presence in the brain in people with HIV with undetectable plasma virus (Sabatier et al., 1991; Cheng et al., 1998; Haughey et al., 2001; Li et al., 2009). This evidence makes it all the more surprising that cocaine and Tat failed to exert additive or synergistic effects on either neurons or astrocytes.

Given that exposure of cells to NMDA largely reflected trends observed from cocaine treatment alone, studies to address similarities among upstream mechanisms for cocaine and NMDA are warranted. In fact, because cocaine, Tat, and NMDA have similar effects, other neurodegenerative diseases including Alzheimer disease, whereby NMDA is implicated as a major contributor to neuronal dysfunction (Malinow 2012, Zhou and Sheng 2013, Avila et al., 2017; Foster et al., 2017; Wang and Reddy 2017, Liu et al., 2019), may show similar changes in lipid metabolism.

Limitations of the study

A possible limitation of our study includes cocaine treatment resulted in significantly more total lipids/cells than Tat alone. However, when cocaine and Tat are given together, the total lipid droplet (LD) number goes back to levels near those observed in Tat alone. We observed a linear correlation between lipid peroxidation and LD accumulation. In addition, our FACS analysis of the conditioned media from Tat or Tat + cocaine shows increased release of lipids in culture media. The increased release of lipids in the culture media explains a decrease in intracellular LD accumulation or lipid peroxidation in neurons treated with Tat or Tat + cocaine. Another possible limitation is that we have not addressed calcium changes in these SCL25A1 KD astrocytes. Given that the sigma receptor-1 plays an important role in organellar and cellular changes in calcium in response to cocaine, we consider these are important future research avenues that will show why there is an increased release of lipids in Tat- or Tat + cocaine-treated neurons compared with cocaine-alone-treated neurons and the impact of the calcium changes.

STAR★METHODS

Detailed methods are provided in the online version of this paper and include the following:

- KEY RESOURCES TABLE
- RESOURCE AVAILABILITY
  - Lead contact
  - Materials availability
  - Data and code availability
- EXPERIMENTAL MODEL AND SUBJECT DETAILS
  - Human primary astrocytes and neurons
  - Rat primary astrocytes and neurons
  - N2a neurons
- METHOD DETAILS
  - Cellular co-cultures and treatments
  - RNAi
  - Mitochondrial reactive oxygen species (mROS) measurement
  - Lipid peroxidation assay
  - Fatty acid transfer assays
  - Lipid staining in neurons/N2A/astrocytes
  - Mitochondrial fatty acid oxidation measurements
  - Western blotting and analyses

- Metabolite analyses of conditioned media and cells
- ATP measurement
- PI staining for cell death assay

- QUANTIFICATION AND STATISTICAL ANALYSIS
  - Statistical analysis

SUPPLEMENTAL INFORMATION

Supplemental information can be found online at https://doi.org/10.1016/j.isci.2022.105407.

ACKNOWLEDGMENTS

This work was National Institutes of Health funded in part by R21DA051798, R00HL138268–04, T32MH079785, P01DA037830, P30MH092177, R556NS124478.

AUTHOR CONTRIBUTIONS

Conceptualization and Project Administration, K.N., S.S., and D.L.; Experimental design and Conducted the Experiments, K.N., S.S., A.G., and D.L.; Software, Data Curation, and Validation, K.N., A.G., and P.V.; Investigation and Formal Analysis, K.N. and S.S.; Writing Original Draft, K.N. and D.L.; Writing, Review & Editing, K.N., S.S., and D.L.; Visualization, K.N., S.S., and P.V.; Computational & Statistics, K.N. and S.S.; Supervision, S.S. and D.L.; Resources and Funding acquisitions, K.N., S.S., and D.L. All co-authors approved the final version of the article and take full responsibility for the accuracy of data and statistical analyses.

DECLARATION OF INTERESTS

The authors declare no competing interests.

Received: November 3, 2021
Revised: August 25, 2022
Accepted: October 17, 2022
Published: November 18, 2022

REFERENCES

Allaman, I., Papp, M., Kraftsik, R., Fiumelli, H., Magistretti, P.J., and Martin, J.L. (2008). Expression of brain-derived neurotrophic factor is not modulated by chronic mild stress in the rat hippocampus and amygdala. Pharmacol. Rep. *60*, 1001–1007.

Avila, J., Llorens-Martín, M., Pallas-Bazarra, N., Bolós, M., Perea, J.R., Rodríguez-Matellán, A., and Hernández, F. (2017). Cognitive decline in neuronal aging and alzheimer's disease: role of NMDA receptors and associated proteins. Front. Neurosci. *11*, 626.

Bailey, A.P., Koster, G., Guillermier, C., Hirst, E.M.A., MacRae, J.I., Lechene, C.P., Postle, A.D., and Gould, A.P. (2015). Antioxidant role for lipid droplets in a stem cell niche of Drosophila. Cell *163*, 340–353.

Bandaru, V.V.R., Mielke, M.M., Sacktor, N., McArthur, J.C., Grant, I., Letendre, S., Chang, L., Wojna, V., Pardo, C., Calabresi, P., et al. (2013). A lipid storage-like disorder contributes to cognitive decline in HIV-infected subjects. Neurology *81*, 1492–1499.

Barber, C.N., and Raben, D.M. (2019). Lipid metabolism crosstalk in the brain: glia and neurons. Front. Cell. Neurosci. *13*, 212.

Bayer, P., Kraft, M., Ejchart, A., Westendorp, M., Frank, R., and Rösch, P. (1995). Structural studies of HIV-1 Tat protein. J. Mol. Biol. *247*, 529–535.

Bélanger, M., Allaman, I., and Magistretti, P.J. (2011). Brain energy metabolism: focus on astrocyte-neuron metabolic cooperation. Cell Metab. *14*, 724–738.

Bélanger, M., and Magistretti, P.J. (2009). The role of astroglia in neuroprotection. Dialogues Clin. Neurosci. *11*, 281–295.

Bodzon-Kulakowska, A., Antolak, A., Drabik, A., Marszalek-Grabska, M., Kotlińska, J., and Suder, P. (2017). Brain lipidomic changes after morphine, cocaine and amphetamine administration - DESI - MS imaging study. Biochim. Biophys. Acta. Mol. Cell Biol. Lipids *1862*, 686–691.

Bolaños, J.P., Almeida, A., and Moncada, S. (2010). Glycolysis: a bioenergetic or a survival pathway? Trends Biochem. Sci. *35*, 145–149.

Boury-Jamot, B., Carrard, A., Martin, J.L., Halfon, O., Magistretti, P.J., and Boutrel, B. (2016). Disrupting astrocyte-neuron lactate transfer persistently reduces conditioned responses to cocaine. Mol. Psychiatry *21*, 1070–1076.

Buch, S., Yao, H., Guo, M., Mori, T., Su, T.P., and Wang, J. (2011). Cocaine and HIV-1 interplay: molecular mechanisms of action and addiction. J. Neuroimmune Pharmacol. *6*, 503–515.

Buydens-Branchey, L., and Branchey, M. (2003). Association between low plasma levels of cholesterol and relapse in cocaine addicts. Psychosom. Med. *65*, 86–91.

Buydens-Branchey, L., Branchey, M., McMakin, D.L., and Hibbeln, J.R. (2003a). Polyunsaturated fatty acid status and aggression in cocaine addicts. Drug Alcohol Depend. *71*, 319–323.

Buydens-Branchey, L., Branchey, M., McMakin, D.L., and Hibbeln, J.R. (2003b). Polyunsaturated fatty acid status and relapse vulnerability in cocaine addicts. Psychiatry Res. *120*, 29–35.

Cheng, J., Nath, A., Knudsen, B., Hochman, S., Geiger, J.D., Ma, M., and Magnuson, D.S. (1998). Neuronal excitatory properties of human immunodeficiency virus type 1 Tat protein. Neuroscience *82*, 97–106.

Cisneros, I.E., Erdenizmenli, M., Cunningham, K.A., Paessler, S., and Dineley, K.T. (2018). Cocaine evokes a profile of oxidative stress and impacts innate antiviral response pathways in astrocytes. Neuropharmacology *135*, 431–443.

Cotto, B., Li, H., Tuma, R.F., Ward, S.J., and Langford, D. (2018a). Cocaine-mediated activation of microglia and microglial MeCP2 and BDNF production. Neurobiol. Dis. *117*, 28–41.

Cotto, B., Natarajanseenivasan, K., and Langford, D. (2019). HIV-1 infection alters energy metabolism in the brain: contributions to

HIV-associated neurocognitive disorders. Prog. Neurobiol. *181*, 101616.

Cotto, B., Natarajaseenivasan, K., Ferrero, K., Wesley, L., Sayre, M., and Langford, D. (2018b). Cocaine and HIV-1 Tat disrupt cholesterol homeostasis in astrocytes: implications for HIV-associated neurocognitive disorders in cocaine user patients. Glia *66*, 889–902.

Cummings, B.S., Pati, S., Sahin, S., Scholpa, N.E., Monian, P., Trinquero, P.M., Clark, J.K., and Wagner, J.J. (2015). Differential effects of cocaine exposure on the abundance of phospholipid species in rat brain and blood. Drug Alcohol Depend. *152*, 147–156.

Deme, P., Rojas, C., Slusher, B.S., Rais, R., Afghah, Z., Geiger, J.D., and Haughey, N.J. (2020). Bioenergetic adaptations to HIV infection. Could modulation of energy substrate utilization improve brain health in people living with HIV-1? Exp. Neurol. *327*, 113181.

Di Noia, M.A., Todisco, S., Cirigliano, A., Rinaldi, T., Agrimi, G., Iacobazzi, V., and Palmieri, F. (2014). The human SLC25A33 and SLC25A36 genes of solute carrier family 25 encode two mitochondrial pyrimidine nucleotide transporters. J. Biol. Chem. *289*, 33137–33148.

Dickens, A.M., Anthony, D.C., Deutsch, R., Mielke, M.M., Claridge, T.D.W., Grant, I., Franklin, D., Rosario, D., Marcotte, T., Letendre, S., et al. (2015). Cerebrospinal fluid metabolomics implicate bioenergetic adaptation as a neural mechanism regulating shifts in cognitive states of HIV-infected patients. AIDS *29*, 559–569.

Dienel, G.A., and Hertz, L. (2001). Glucose and lactate metabolism during brain activation. J. Neurosci. Res. *66*, 824–838.

Donadelli, M., Dando, I., Fiorini, C., and Palmieri, M. (2014). UCP2, a mitochondrial protein regulated at multiple levels. Cell. Mol. Life Sci. *71*, 1171–1190.

Ernst, T., Chang, L., and Arnold, S. (2003). Increased glial metabolites predict increased working memory network activation in HIV brain injury. Neuroimage *19*, 1686–1693.

Farese, R.V., Jr., and Walther, T.C. (2009). Lipid droplets finally get a little R-E-S-P-E-C-T. Cell *139*, 855–860.

Farmer, B.C., Walsh, A.E., Kluemper, J.C., and Johnson, L.A. (2020). Lipid droplets in neurodegenerative disorders. Front. Neurosci. *14*, 742.

Fernandez, H.R., Gadre, S.M., Tan, M., Graham, G.T., Mosaoa, R., Ongkeko, M.S., Kim, K.A., Riggins, R.B., Parasido, E., Petrini, I., et al. (2018). The mitochondrial citrate carrier, SLC25A1, drives stemness and therapy resistance in non-small cell lung cancer. Cell Death Differ. *25*, 1239–1258.

Foster, T.C., Kyritsopoulos, C., and Kumar, A. (2017). Central role for NMDA receptors in redox mediated impairment of synaptic function during aging and Alzheimer's disease. Behav. Brain Res. *322*, 223–232.

Giangregorio, N., Console, L., Tonazzi, A., Palmieri, F., and Indiveri, C. (2014). Identification of amino acid residues underlying the antiport mechanism of the mitochondrial carnitine/acylcarnitine carrier by site-directed mutagenesis and chemical labeling. Biochemistry *53*, 6924–6933.

Guo, Y., Cordes, K.R., Farese, R.V., Jr., and Walther, T.C. (2009). Lipid droplets at a glance. J. Cell Sci. *122*, 749–752.

Haughey, N.J., Cutler, R.G., Tamara, A., McArthur, J.C., Vargas, D.L., Pardo, C.A., Turchan, J., Nath, A., and Mattson, M.P. (2004). Perturbation of sphingolipid metabolism and ceramide production in HIV-dementia. Ann. Neurol. *55*, 257–267.

Haughey, N.J., Nath, A., Mattson, M.P., Slevin, J.T., and Geiger, J.D. (2001). HIV-1 Tat through phosphorylation of NMDA receptors potentiates glutamate excitotoxicity. J. Neurochem. *78*, 457–467.

Hirsch-Reinshagen, V., Zhou, S., Burgess, B.L., Bernier, L., McIsaac, S.A., Chan, J.Y., Tansley, G.H., Cohn, J.S., Hayden, M.R., and Wellington, C.L. (2004). Deficiency of ABCA1 impairs apolipoprotein E metabolism in brain. J. Biol. Chem. *279*, 41197–41207.

Hu, X.T. (2016). HIV-1 tat-mediated calcium dysregulation and neuronal dysfunction in vulnerable brain regions. Curr. Drug Targets *17*, 4–14.

Infantino, V., Iacobazzi, V., De Santis, F., Mastrapasqua, M., and Palmieri, F. (2007). Transcription of the mitochondrial citrate carrier gene: role of SREBP-1, upregulation by insulin and downregulation by PUFA. Biochem. Biophys. Res. Commun. *356*, 249–254.

Infantino, V., Iacobazzi, V., Menga, A., Avantaggiati, M.L., and Palmieri, F. (2014). A key role of the mitochondrial citrate carrier (SLC25A1) in TNFalpha- and IFNgamma-triggered inflammation. Biochim. Biophys. Acta *1839*, 1217–1225.

Ioannou, M.S., Jackson, J., Sheu, S.H., Chang, C.L., Weigel, A.V., Liu, H., Pasolli, H.A., Xu, C.S., Pang, S., Matthies, D., et al. (2019). Neuron-astrocyte metabolic coupling protects against activity-induced fatty acid toxicity. Cell *177*, 1522–1535.e14.

Ioannou, M.S., Jackson, J., Sheu, S.-H., Chang, C.-L., Weigel, H.L.A.V., Amalia Pasolli, H., Shan Xu, C., Song, P., Harald, J.L.-S., Hess, F., and Liu, Z. (2018). Neuron-astrocyte metabolic coupling during neuronal stimulation protects against fatty acid toxicity. Preprint at bioRxiv. https://doi.org/10.1101/465237.

Islam, A., Kagawa, Y., Miyazaki, H., Shil, S.K., Umaru, B.A., Yasumoto, Y., Yamamoto, Y., and Owada, Y. (2019). FABP7 protects astrocytes against ROS toxicity via lipid droplet formation. Mol. Neurobiol. *56*, 5763–5779.

Jaeger, L.B., and Nath, A. (2012). Modeling HIV-associated neurocognitive disorders in mice: new approaches in the changing face of HIV neuropathogenesis. Dis. Model. Mech. *5*, 313–322.

Keren-Shaul, H., Spinrad, A., Weiner, A., Matcovitch-Natan, O., Dvir-Szternfeld, R., Ulland, T.K., David, E., Baruch, K., Lara-Astaiso, D., Toth, B., et al. (2017). A unique microglia type Associated with restricting development of alzheimer's disease. Cell *169*, 1276–1290.e17.

Kovalevich, J., Corley, G., Yen, W., Rawls, S.M., and Langford, D. (2012a). Cocaine-induced loss of white matter proteins in the adult mouse nucleus accumbens is attenuated by administration of a beta-lactam antibiotic during cocaine withdrawal. Am. J. Pathol. *181*, 1921–1927.

Kovalevich, J., Corley, G., Yen, W., Kim, J., Rawls, S.M., and Langford, D. (2012b). Cocaine decreases expression of neurogranin via alterations in thyroid receptor/retinoid X receptor signaling. J. Neurochem. *121*, 302–313.

Kovalevich, J., Yen, W., Ozdemir, A., and Langford, D. (2015). Cocaine induces nuclear export and degradation of neuronal retinoid X receptor-γ via a TNF-α/JNK- mediated mechanism. J. Neuroimmune Pharmacol. *10*, 55–73 in press.

Kwon, Y.H., Kim, J., Kim, C.S., Tu, T.H., Kim, M.S., Suk, K., Kim, D.H., Lee, B.J., Choi, H.S., Park, T., et al. (2017). Hypothalamic lipid-laden astrocytes induce microglia migration and activation. FEBS Lett. *591*, 1742–1751.

Li, W., Li, G., Steiner, J., and Nath, A. (2009). Role of Tat protein in HIV neuropathogenesis. Neurotox. Res. *16*, 205–220.

Lin, Y., Gu, H., Jiang, L., Xu, W., Liu, C., Li, Y., Qian, X., Li, D., Li, Z., Hu, J., et al. (2017a). Cocaine modifies brain lipidome in mice. Mol. Cell. Neurosci. *85*, 29–44.

Liu, J., Chang, L., Song, Y., Li, H., and Wu, Y. (2019). The role of NMDA receptors in alzheimer's disease. Front. Neurosci. *13*, 43.

Liu, L., Mackenzie, K.R., Putluri, N., Maletic-Savatic, M., and Bellen, H.J. (2017b). The glia-Neuron lactate shuttle and elevated ROS promote lipid synthesis in neurons and lipid droplet accumulation in Glia via APOE/D. Cell Metab. *26*, 719–737.

Liu, L., Zhang, K., Sandoval, H., Yamamoto, S., Jaiswal, M., Sanz, E., Li, Z., Hui, J., Graham, B.H., Quintana, A., and Bellen, H.J. (2015). Glial lipid droplets and ROS induced by mitochondrial defects promote neurodegeneration. Cell *160*, 177–190.

Loving, B.A., and Bruce, K.D. (2020). Lipid and lipoprotein metabolism in microglia. Front. Physiol. *11*, 393.

Magistretti, P.J. (2006). Neuron-glia metabolic coupling and plasticity. J. Exp. Biol. *209*, 2304–2311.

Malinow, R. (2012). New developments on the role of NMDA receptors in Alzheimer's disease. Curr. Opin. Neurobiol. *22*, 559–563.

Marcondes, M.C., Burudi, E.M., Huitron-Resendiz, S., Sanchez-Alavez, M., Watry, D., Zandonatti, M., Henriksen, S.J., and Fox, H.S. (2001). Highly activated CD8(+) T cells in the brain correlate with early central nervous system dysfunction in simian immunodeficiency virus infection. J. Immunol. *167*, 5429–5438.

Marschallinger, J., Iram, T., Zardeneta, M., Lee, S.E., Lehallier, B., Haney, M.S., and al, e. (2020).

Lipid-droplet-accumulating microglia represent a dysfunctional and proinflammatory state in the aging brain. Nat. Neurosci. *23*, 194–208.

Meng, H., Wang, M., Liu, H., Liu, X., Situ, A., Wu, B., et al. (2015). Use of a Lipidcoated mesoporous silica nanoparticle platform for synergistic gemcitabine and paclitaxel, delivery to human pancreatic cancer in mice. ACS Nano *9*, 3540–3557.

Mielke, M.M., Bandaru, V.V.R., McArthur, J.C., Chu, M., and Haughey, N.J. (2010). Disturbance in cerebral spinal fluid sphingolipid content is associated with memory impairment in subjects infected with the human immunodeficiency virus. J. Neurovirol. *16*, 445–456.

Mohseni Ahooyi, T., Shekarabi, M., Torkzaban, B., Langford, T.D., Burdo, T.H., Gordon, J., Datta, P.K., Amini, S., and Khalili, K. (2018). Dysregulation of neuronal cholesterol homeostasis upon exposure to HIV-1 tat and cocaine revealed by RNA-sequencing. Sci. Rep. *8*, 16300–16313.

Mosaoa, R., Kasprzyk-Pawelec, A., Fernandez, H.R., and Avantaggiati, M.L. (2021). The mitochondrial citrate carrier SLC25A1/CIC and the fundamental role of citrate in cancer, inflammation and beyond. Biomolecules *11*, 141.

Natarajaseenivasan, K., Cotto, B., Shanmughapriya, S., Lombardi, A.A., Datta, P.K., Madesh, M., Elrod, J.W., Khalili, K., and Langford, D. (2018). Astrocytic metabolic switch is a novel etiology for Cocaine and HIV-1 Tat-mediated neurotoxicity. Cell Death Dis. *9*, 415.

Nath, A. (2002). Human immunodeficiency virus (HIV) proteins in neuropathogenesis of HIV dementia. J. Infect. Dis. *186*, S193–S198.

Nogueiras, R., Tschöp, M.H., and Zigman, J.M. (2008). Central nervous system regulation of energy metabolism: ghrelin versus leptin. Ann. N. Y. Acad. Sci. *1126*, 14–19.

Ortinski, P.I. (2014). Cocaine-induced changes in NMDA receptor signaling. Mol. Neurobiol. *50*, 494–506.

Palmieri, F. (2013). The mitochondrial transporter family SLC25: identification, properties and physiopathology. Mol. Aspects Med. *34*, 465–484.

Pennetta, G., and Welte, M.A. (2018). Emerging links between lipid droplets and motor neuron diseases. Dev. Cell *45*, 427–432.

Purohit, V., Rapaka, R., and Shurtleff, D. (2011). Drugs of abuse, dopamine, and HIV-associated neurocognitive disorders/HIV-associated dementia. Mol. Neurobiol. *44*, 102–110.

Ratai, E.M., Annamalai, L., Burdo, T., Joo, C.G., Bombardier, J.P., Fell, R., Hakimelahi, R., He, J., Lentz, M.R., Campbell, J., et al. (2011). Brain creatine elevation and N-Acetylaspartate reduction indicates neuronal dysfunction in the setting of enhanced glial energy metabolism in a macaque model of neuroAIDS. Magn. Reson. Med. *66*, 625–634.

Ross, B.M., Moszczynska, A., Peretti, F.J., Adams, V., Schmunk, G.A., Kalasinsky, K.S., Ang, L., Mamalias, N., Turenne, S.D., and Kish, S.J. (2002). Decreased activity of brain phospholipid metabolic enzymes in human users of cocaine and methamphetamine. Drug Alcohol Depend. *67*, 73–79.

Sabatier, J.M., Vives, E., Mabrouk, K., Benjouad, A., Rochat, H., Duval, A., Hue, B., and Bahraoui, E. (1991). Evidence for neurotoxic activity of tat from human immunodeficiency virus type 1. J. Virol. *65*, 961–967.

Sanna, P.P., Fu, Y., Masliah, E., Lefebvre, C., and Repunte-Canonigo, V. (2021). Central nervous system (CNS) transcriptomic correlates of human immunodeficiency virus (HIV) brain RNA load in HIV-infected individuals. Sci. Rep. *11*, 12176.

Schönfeld, P., and Reiser, G. (2013). Why does brain metabolism not favor burning of fatty acids to provide energy? Reflections on disadvantages of the use of free fatty acids as fuel for brain. J. Cereb. Blood Flow Metab. *33*, 1493–1499.

Shao, X., Tang, Y., Long, H., Gu, H., Zhang, J., Deng, P., Zhao, Y., and Cen, X. (2019). HMG-CoA synthase 2 drives brain metabolic reprogramming in cocaine exposure. Neuropharmacology *148*, 377–393.

Shimabukuro, M.K., Langhi, L.G.P., Cordeiro, I., Brito, J.M., Batista, C.M.d.C., Mattson, M.P., and Mello Coelho, V.d. (2016). Lipid-laden cells differentially distributed in the aging brain are functionally active and correspond to distinct phenotypes. Sci. Rep. *6*, 23795.

Sivalingam, K., Cirino, T.J., McLaughlin, J.P., and Samikkannu, T. (2021). HIV-tat and cocaine impact brain energy metabolism: redox modification and mitochondrial biogenesis influence NRF transcription-mediated neurodegeneration. Mol. Neurobiol. *58*, 490–504.

Sultana, R., Perluigi, M., and Butterfield, D.A. (2013). Lipid peroxidation triggers neurodegeneration: a redox proteomics view into the Alzheimer disease brain. Free Radic. Biol. Med. *62*, 157–169.

Suzuki, A., Stern, S.A., Bozdagi, O., Huntley, G.W., Walker, R.H., Magistretti, P.J., and Alberini, C.M. (2011). Astrocyte-neuron lactate transport is required for long-term memory formation. Cell *144*, 810–823.

Teixeira, V., Maciel, P., and Costa, V. (2021). Leading the way in the nervous system: lipid Droplets as new players in health and disease. Biochim. Biophys. Acta. Mol. Cell Biol. Lipids *1866*, 158820.

Tsacopoulos, M., and Magistretti, P.J. (1996). Metabolic coupling between glia and neurons. J. Neurosci. *16*, 877–885.

Tyagi, M., Weber, J., Bukrinsky, M., and Simon, G.L. (2016). The effects of cocaine on HIV transcription. J. Neurovirol. *22*, 261–274.

Volkow, N.D., Fowler, J.S., Wang, G.J., Hitzemann, R., Logan, J., Schlyer, D.J., Dewey, S.L., and Wolf, A.P. (1993). Decreased dopamine D2 receptor availability is associated with reduced frontal metabolism in cocaine abusers. Synapse *14*, 169–177.

Volkow, N.D., Fowler, J.S., Wang, G.J., Telang, F., Logan, J., Jayne, M., Ma, Y., Pradhan, K., Wong, C., and Swanson, J.M. (2010). Cognitive control of drug craving inhibits brain reward regions in cocaine abusers. Neuroimage *49*, 2536–2543.

Volkow, N.D., Fowler, J.S., Wolf, A.P., Schlyer, D., Shiue, C.Y., Alpert, R., Dewey, S.L., Logan, J., Bendriem, B., Christman, D., et al. (1990). Effects of chronic cocaine abuse on postsynaptic dopamine receptors. Am. J. Psychiatry *147*, 719–724.

Walther, T.C., and Farese, R.V., Jr. (2009). The life of lipid droplets. Biochim. Biophys. Acta *1791*, 459–466.

Wang, R., and Reddy, P.H. (2017). Role of glutamate and NMDA receptors in alzheimer's disease. J. Alzheimers Dis. *57*, 1041–1048.

Westendorp, M.O., Shatrov, V.A., Schulze-Osthoff, K., Frank, R., Kraft, M., Los, M., Krammer, P.H., Dröge, W., and Lehmann, V. (1995). HIV-1 Tat potentiates TNF-induced NF-kappa B activation and cytotoxicity by altering the cellular redox state. EMBO J. *14*, 546–554.

Westergaard, N., Waagepetersen, H.S., Belhage, B., and Schousboe, A. (2017). Citrate, a ubiquitous key metabolite with regulatory function in the cns. Neurochem. Res. *42*, 1583–1588.

Williams, M.E., Naudé, P.J.W., and van der Westhuizen, F.H. (2021). Proteomics and metabolomics of HIV-associated neurocognitive disorders: a systematic review. J. Neurochem. *157*, 429–449.

Xiao, H., Neuveut, C., Tiffany, H.L., Benkirane, M., Rich, E.A., Murphy, P.M., and Jeang, K.T. (2000). Selective CXCR4 antagonism by Tat: implications for in vivo expansion of coreceptor use by HIV-1. Proc. Natl. Acad. Sci. USA *97*, 11466–11471.

Xie, Y., Li, J., Kang, R., and Tang, D. (2020). Interplay between lipid metabolism and autophagy. Front. Cell Dev. Biol. *8*, 431.

Yassine, H.N., Feng, Q., Chiang, J., Petrosspour, L.M., Fonteh, A.N., Chui, H.C., and Harrington, M.G. (2016). ABCA1-Mediated cholesterol efflux capacity to cerebrospinal fluid is reduced in patients with mild cognitive impairment and alzheimer's disease. J. Am. Heart Assoc. *5*, e002886.

Young, A.C., Yiannoutsos, C.T., Hegde, M., Lee, E., Peterson, J., Walter, R., Price, R.W., Meyerhoff, D.J., and Spudich, S. (2014). Cerebral metabolite changes prior to and after antiretroviral therapy in primary HIV infection. Neurology *83*, 1592–1600.

Zhou, Q., and Sheng, M. (2013). NMDA receptors in nervous system diseases. Neuropharmacology *74*, 69–75.

STAR★METHODS

KEY RESOURCES TABLE

REAGENT or RESOURCE	SOURCE	IDENTIFIER
Antibodies		
GFAP	Cell Signaling Technology	Cat# 3670S; RRID: AB_561049
MAP2	Cell Signaling Technology	Cat# 4542S; RRID: AB_10693782
Iba-1	Wako	Cat# 016-20001: RRID: AB_839506
SLC25A1	Thermo Fisher Scientific	Cat# 15235-1-AP; RRID: AB_2254794
PSD95	Abcam	Cat# ab18258; RRID: AB_444362
LXRα-β	Santa Cruz Biotechnology	Cat# sc-377260
β-Actin	Santa Cruz Biotechnology	Cat# sc-47778
LDLR	Santa Cruz Biotechnology	Cat# sc-18823; RRID: AB_627881
LC3BI and LC3BII	Sigma-Aldrich	Cat# SAB5700049
pAMPK	Cell Signaling Technology	Cat# 2535S; RRID: AB_331250
AMPK	Cell Signaling Technology	Cat# 2532S; RRID: AB_331250
Chemicals, peptides, and recombinant proteins		
HBSS	Thermo Fisher Scientific	Cat# 14175095
Trypsin	Thermo Fisher Scientific	Cat# 25200056
Papain	Sigma-Aldrich	Cat# P4762
FBS	Thermo Fisher Scientific	Cat# 12483020
DMEM: F12	Thermo Fisher Scientific	Cat# 10565018
L-glutamine	Thermo Fisher Scientific	Cat# A1286001
Gentamicin	Thermo Fisher Scientific	Cat# 15710064
Insulin	Sigma-Aldrich	Cat# I2643
B-27	Thermo Fisher Scientific	Cat# 17504044
Horse serum	Thermo Fisher Scientific	Cat# 16050122
Neurobasal media	Thermo Fisher Scientific	Cat# 21103049
Poly-D-lysine	Sigma-Aldrich	Cat# P6407
5-fluorodeoxyuridine (FDU)	Sigma-Aldrich	Cat# F0503
Uridine	Sigma-Aldrich	Cat# U3750
MEM	Thermo Fisher Scientific	Cat# 11095080
Retinoic acid	Sigma-Aldrich	Cat# R2625
Tat	ImmunoDX	Cat# 1032
Cocaine	Sigma-Aldrich	Cat# C5776
NMDA	Sigma-Aldrich	Cat# M3262
α-tocopherol	Thermo Fisher Scientific	Cat# 421031000
siRNA (SLC25A1)	Horizon Discovery Biosciences Limited	Cat# L-007468
MitoSOX Red	Thermo Fisher Scientific	Cat# N36008
BODIPY® 493/503	Thermo Fisher Scientific	Cat# D3922
BODIPY 581/591 C11	Thermo Fisher Scientific	Cat# D3861
BODIPY 558/568 C12	Thermo Fisher Scientific	Cat# D3835
Rhodamine 123	Thermo Fisher Scientific	Cat# R302
Palmitate	Sigma-Aldrich	Cat# P0500
BSA	Sigma-Aldrich	Cat# A9418

(*Continued on next page*)

Continued

REAGENT or RESOURCE	SOURCE	IDENTIFIER
Etomoxir	Sigma-Aldrich	Cat# E1905
Oligomycin	Agilent Technologies	Cat# 103015-100
FCCP	Agilent Technologies	Cat# 103015-100
Rotenone	Agilent Technologies	Cat# 103015-100
Antimycin A	Agilent Technologies	Cat# 103015-100
RIPA buffer	Thermo Fisher Scientific	Cat# 89900
Complete protease inhibitor cocktail	Thermo Fisher Scientific	Cat# 87785
Halt phosphatase inhibitor cocktail	Thermo Fisher Scientific	Cat# 78420
4-12% Bis-Tris polyacrylamide gel	Thermo Fisher Scientific	Cat# WG1402A
iBlot 2 NC regular stacks	Thermo Fisher Scientific	Cat# IB23001
Hoechst 33342	Thermo Fisher Scientific	Cat# H21492
Propidium iodide	Thermo Fisher Scientific	Cat# J66764-MC
Critical commercial assays		
Lactate	Sigma-Aldrich	Cat# MAK064
LDH	Sigma-Aldrich	Cat# MAK066
Extracellular cholesterol	Invitrogen	Cat# A12216
Intracellular cholesterol	Abcam	Cat# ab133116
Apolipoprotein E human ELISA kit	Thermo Fisher Scientific	Cat# EHAPOE
CellTiter-Glo luminescent assay	Promega	Cat# G7570
Experimental models: Cell lines		
Human astrocytes	Comprehensive NeuroAIDS Center at Temple University	N/A
Human neurons	Comprehensive NeuroAIDS Center at Temple University	N/A
Rat astrocytes	Comprehensive NeuroAIDS Center at Temple University	N/A
Rat neurons	Comprehensive NeuroAIDS Center at Temple University	N/A
Software and algorithms		
ImageJ	NIH	https://imagej.nih.gov/ij
Prism statistics	GraphPad	Version 9.4.1
SigmaPlot	Spw	Version 11.0

RESOURCE AVAILABILITY

Lead contact

Further information and requests for reagents and resources may be directed to and will be fulfilled by the lead contact, Dr. Dianne Langford (Dianne.langford@temple.edu).

Materials availability

This study did not generate new unique reagents.

Data and code availability

- The original data reported in this paper is available from the lead contact upon request.
- This paper does not report original code.
- Any additional information required to reanalyze the data reported in this paper is available from the lead contact upon request.

EXPERIMENTAL MODEL AND SUBJECT DETAILS

Human primary astrocytes and neurons

Human primary astrocytes and neurons were obtained from the Comprehensive NeuroAIDS Center at Temple University, as previously described (Cotto et al., 2018b; Natarajaseenivasan et al., 2018). Human fetal brain tissue (gestational age, 16–18 weeks) was obtained from elective abortion procedures performed in full compliance with National Institutes of Health and Temple University human subjects board guidelines. Briefly, the tissue was washed with cold Hanks balanced salt solution (HBSS), and meninges and blood vessels were removed. Tissue in HBSS was digested with 0.25% trypsin (Sigma Chemical Co., St. Louis, Mo.) or papain (20 mg/ml) for 30 min at 37°C for isolation of glia or neurons, respectively. The digestion was neutralized with fetal bovine serum (FBS), and the tissue was further dissociated to obtain single-cell suspensions. For glial cultures, cells were plated in mixed glial growth media (DMEM:F12 media supplemented with insulin, FBS, L-glutamine, and gentamicin). The mixed culture was maintained under at 37ºC 5% CO_2 for 5 days at which time the media was replaced. To enrich for astrocytes, flasks were placed on an orbital shaker for 14–18 h at 200 rpm at 37ºC 5% CO_2. Detached cells constituted the microglial component of the culture and were removed. Astrocytes that remained after shaking were fed with astrocyte media consisting of DMEM:F12 media supplemented with insulin, FBS, L-glutamine, and gentamicin. Purity of astrocytes were confirmed by immunocytochemical (ICC) labeling with anti-glial fibrillary acid protein (GFAP) and lack of MAP2 or neurofilament. For neurons, the tissue was washed with HBSS, resuspended in NM5 media (neurobasal media supplemented with 5% horse serum, 1% B27, 1% glutamax, gentamycin), and further dissociated by repeated pipetting to obtain single-cell suspensions. The cell suspension was passed through a 70-micron cell strainer and cells were counted. The single-cell suspension was plated at a density of ~3.0×10^6 cells/poly-D lysine coated 60 mm dish in NM5 media. Twenty-four hours later, cultures were refed with a complete change of neurobasal media without horse serum (NM0). Four days later, half of the media was removed and replaced with neurobasal media (NM0) supplemented with 1.25uM FDU and 1.5uM uridine. Purity of cultures was assessed by immunolabeling with antibodies for MAP2, GFAP, and Iba-1.

Rat primary astrocytes and neurons

Animal care and experimental procedures were conducted according to the Guide for the Care and Use of Laboratory Animals. The Institutional Animal Care and Use Committee of Temple University approved experimental protocols. Brain tissue was harvested from embryonic day 15-18 Sprague–Dawley rat embryos. For glial cultures, cells were plated in mixed glial growth media (DMEM:F12 media supplemented with insulin, FBS, L-glutamine, and gentamicin). The mixed culture was maintained under at 37ºC 5% CO_2 for 5 days at which time the media was replaced. To enrich for astrocytes, flasks were placed on an orbital shaker for 14–18 h at 200 rpm at 37ºC 5% CO_2. Detached cells constituted the microglial component of the culture and were removed. Astrocytes that remained after shaking were fed with astrocyte media consisting of DMEM:F12 media supplemented with insulin, FBS, L-glutamine, and gentamicin. Purity of astrocytes were confirmed by immunocytochemical (ICC) labeling with anti-glial fibrillary acid protein (GFAP) and lack of MAP2 or neurofilament. To enrich for neurons, a single-cell suspension was plated at a density of approximately 1.8×10^6 cells/60 mm dish coated with poly-D lysine in neurobasal media with B27 supplement, horse serum, and gentamicin (NM5). After approximately 2h, media was removed and neurons were refed with neurobasal media. Twenty-four hours later, cultures were refed with a complete change of neurobasal media lacking horse serum (NM0). Four days later, one-fourth of the media was removed and replaced with neurobasal media (NM0) supplemented with 5-fluorodeoxyuridine (FDU). Purity of neurons was confirmed by ICC labeling with anti-MAP2/neurofilament (neurons) or lack of GFAP labeling.

N2a neurons

The mouse neuroblastoma cell line Neuro-2a (ATCC CCL131) cells were grown in Modified Eagle Medium (MEM; Corning), supplemented with 10% fetal bovine serum (HyClone) and 1% antibiotic antimycotic solution (10,000 units penicillin, 10 mg streptomycin and 25 mg amphotericin B/mL; Sigma-Aldrich, USA). For cell differentiation, approximately 18h after initial plating, complete media was replaced with MEM differentiation media containing 2% FBS, 20 μM retinoic acid and 1% antibiotic antimycotic solution. The cells were incubated with differentiating media for 72h and ICC confirmation before experiments were conducted.

METHOD DETAILS

Cellular co-cultures and treatments

Rat primary neurons or N2a neurons were exposed to 50 ng/mL recombinant Tat (rTat, ImmunoDX LLC, Woburn, WA) and/or 5 μM cocaine hydrochloride (Sigma-Aldrich) for 48h. Primary neurons or N2a not exposed to Tat or cocaine served as controls. In some experiments, rat neurons were treated with NMDA (100 μM) for 4 h as a positive control for lipid accumulation and peroxidation (Ioannou et al., 2019) or α-tocopherol (50 μM) was used to quench reactive oxygen species. In some experiments, rat neurons were cultured onto 0.4μm pore *trans*well inserts (COSTAR Corning, Kennebunk, ME) and rat astrocytes were cultured on the plate below, where cells could communicate via soluble factors, but direct contact was prevented as previously described (Cotto et al., 2018b; Natarajaseenivasan et al., 2018). Using the *trans*well system, neurons cultured onto the transwell filter were exposed to Tat/cocaine.

RNAi

Astrocytes (0.5 × 10^6/well) grown on six-well plates were transfected with pools of 5 distinct siRNAs against SLC25A1 (ON-TARGETplus SMARTpool, Dharmacon, USA) (50 nM) using RNAiMAX transfection reagent (ThermoScientific). As a control, non-targeting/scrambled siRNA (Scr siRNA) duplexes (Dharmacon) were used. Forty-eight hours post-transfection, the cells were exposed to control neuronal conditioned media or media from neurons exposed to Tat/cocaine for 16h.

Mitochondrial reactive oxygen species (mROS) measurement

Rat primary neurons or N2a neurons were plated on Poly-D-lysine coated glass coverslips. Neurons were exposed to 50 ng/mL rTat and/or 5 μM cocaine hydrochloride for 48h either in the presence or absence of α-tocopherol (50 μM). Neurons exposed to NMDA (100 μM) for 4h or neurons with no treatment were used as controls. After 4h NMDA, no treatment control or 48h Tat/coc neurons were loaded with the mitochondrial superoxide sensitive fluorophore MitoSOX Red (Life Technologies; 5 μM) in NM0 or MEM medium at 37ºC for 30 min. Neurons were then washed and imaged using a Carl Zeiss LSM 810 with a 63× oil immersion objective at 561 nm as described previously. MitoSOX fluorescence was quantified using Graph software and plotted as arbitrary units in GraphPad Prism 9 software. For MitoSOX fluorescence was quantified on ImageJ using Oval elliptical or brush selection. Approximately 5 oval spots/cell were quantified for fluorescence intensity and analyzed.

Lipid peroxidation assay

For the lipid hydroperoxide assay, rat neurons were grown on Poly-D-lysine coated glass coverslips. Cells were exposed to 50 ng/mL Tat and/or 5 μM cocaine hydrochloride for 48h or NMDA (100 μM) for 4h with or without α-tocopherol (50 μM). Untreated neurons were used as controls. After appropriate incubation times, neurons were stained with BODIPY 581/591 C11 (2 μM) in NM0/MEM medium for 30 min at 37ºC. Neurons were then washed and imaged using a Carl Zeiss LSM 810 with a 63× oil immersion objective at 591 and 488 nm, as described previously (Ioannou et al., 2019). Relative lipid peroxidation was detected by the ratio of green fluorescence intensity over red fluorescence intensity from background subtracted images using ImageJ software for analyses.

Fatty acid transfer assays

Rat neurons exposed to Tat/cocaine/NMDA were incubated with BODIPY 558/568 C12 (Red-C12) (2 μM) for 16 h. After 16h of incubation, the cell-free neuronal media were collected and analyzed using flow cytometry (Guava easyCyte Flow Cytometer) to quantify the transfer of fatty acids to the extracellular media. Standard FACS analysis was performed using a 561 nm laser. FACS analysis was performed using an unstained media control for determining appropriate gates. The concentration of Red C-12 positive particles was plotted on a logarithmic scale using Flow-Jo software. Astrocytes plated on 0.2% gelatin coated glass coverslips were exposed to neuronal conditioned media for 16 h. After 16 h astrocytes were loaded with Rhodamine 123 (1 μM) at 37ºC for 30 min to stain astrocytic mitochondria. Cells were then washed and imaged using a Carl Zeiss LSM 810 with a 63× oil immersion objective at 488 and 561 nm. The number of Red- C12 positive lipid droplets per astrocyte was quantified and plotted in GraphPad Prism 9 software.

Lipid staining in neurons/N2A/astrocytes

Rat neurons were cultured on Poly-D-lysine (for neurons) coated glass coverslips. Neurons were exposed to 50 ng/mL recombinant Tat (rTat, ImmunoDX LLC, Woburn, WA) and/or 5 μM cocaine hydrochloride

(Sigma-Aldrich) for 48 h. Neurons exposed to NMDA (100 μM) for 4 h or cells with no treatment were used as controls. Scr siRNA and SLC25A1 KD astrocytes cultured on 0.2% gelatin coated glass coverslips were exposed to neuronal conditioned media for 16h and cells with no treatment were used as controls. After the specified incubation time, control and treated neurons/N2A/astrocytes were loaded with BODIPY 493/503 (1 μg/mL) in NM0/MEM/medium for 30 min. Cells were washed and images were acquired using a Carl Zeiss 810 confocal microscope using a 63× oil objective at 488 nm. Images were quantified for the size and number of lipid droplets using ImageJ software.

Mitochondrial fatty acid oxidation measurements

Neurons or astrocytes were plated in Poly-D-lysine coated 96 well Seahorse culture plates. Oxygen consumption rate (OCR) was measured at 37ºC in an XF96 extracellular flux analyzer (Seahorse Bioscience). For the measurement of FAO coupled OCR, cells were glucose depleted overnight and exogenous palmitate (1mM) was used as fatty acid substrate for the OCR measurement. Carnitine palmitoyl transferase-1 inhibitor, Etomoxir (40 μM) was also used to monitor endogenous fatty acid utilization. Neurons, N2A or astrocytes were sequentially challenged with 2 μM oligomycin, 0.5 μM FCCP, and 0.5 μM rotenone plus antimycin A at indicated time points to measure basal and maximal respiration, ATP production, proton leak, spare respiratory capacity, and non-mitochondrial respiration as described (Natarajaseenivasan et al., 2018).

Western blotting and analyses

Cell extracts were prepared from neurons and from astrocytes using RIPA buffer (50 mM Tris-HCl, pH 7.4, 150 mM NaCl, 0.25% deoxycholic acid, 1 mM EDTA, 1% NP-40, protease inhibitor cocktail (Complete, Roche), and Halt phosphatase inhibitor cocktail (Thermo Scientific). Equal amounts of protein (25 μg/lane) were separated on 4–12% Bis-Tris polyacrylamide gel, transferred to a nitrocellulose membrane using iBlot 2 NC regular stacks (Thermo Scientific), and probed with antibodies specific for SLC25A1 (1:500, Invitrogen), MAP2 (1:1000, Cell Signaling), PS D95 (1:1000, Abcam), β-actin (1:4000, Santa Cruz), LXRα-β (1:500, Santa Cruz), and LDLR (1:500, Santa Cruz). For detection of autophagy induction neuronal lysates were prepared and immunoblotted with antibodies specific for LC3Bland LCBII (1:5000, Sigma-Aldrich), pAMPK (1:1000, Cell Signaling), and AMPK (1:1000, Cell Signaling), as described above.

Metabolite analyses of conditioned media and cells

Lactate (MAK064, Sigma-Aldrich), LDH (MAK066, Sigma-Aldrich), extracellular cholesterol (Amplex red cholesterol assay kit A12216, Invitrogen), intracellular cholesterol (cholesterol assay kit, cell-based, ab133116 Abcam), and ApoE (Apolipoprotein E human ELISA kit, EHAPOE, Invitrogen) concentrations or activity in media or in cells were measured following the manufacturer's instructions.

ATP measurement

Total ATP was assessed in neurons and astrocytes using the CellTiter-Glo luminescent assay (Promega) according to the manufacturer's instructions and as described previously (Natarajaseenivasan et al., 2018).

PI staining for cell death assay

Cells grown on poly-D-lysine or 0.2% gelatin coated coverslips and exposed to Tat and/or cocaine (neurons) or neuronal conditioned media (astrocytes) were loaded Hoechst 33,342 (100 μg/mL) and propidium iodide (0.5 μg/mL) for 10 min in NM0/MEM/astrocyte media at 37ºC. Images were acquired with a Carl Zeiss 810 LSM using a 63× oil objective at 405 and 561 nm. Images were quantified for percentages of PI positive cells using ImageJ software.

QUANTIFICATION AND STATISTICAL ANALYSIS

Statistical analysis

Data from multiple experiments (≥ 3) were quantified and expressed as Mean $\pm$ SE, and differences between groups were analyzed using the two-tailed paired Student's *t* test or, when not normally distributed, a nonparametric Mann–Whitney U-test (Wilcoxon Rank-Sum Test) for two groups. Differences in means among multiple datasets were analyzed using one-way ANOVA with Tukey correction performed. A $p \leq 0.05$ was considered significant in all analyses. The data were computed either with GraphPad Prism version 9.0 or SigmaPlot 11.0 software.